antioxidants

MDPI

Article

Chlorogenic Acid Improves Porcine Oocyte Maturation and Post-Warming Survival Accompanied by Mitochondrial and Antioxidant Changes

Kelin Song [1,2], Li Wang [1], Feng Yang [1], Qiuyu Meng [1], Kexin Luo [1], Yiwen Kong [1], Xuelei Han [1], Shuangbao Gun [2], Xinjian Li [1,3,4,*] and Tong Yu [1,*]

[1] College of Animal Science and Technology, Henan Agricultural University, Zhengzhou 450002, China; 17899312494@163.com (K.S.); 18338155530@163.com (L.W.); chinafy6868@163.com (F.Y.); 13629929273@163.com (Q.M.); 18348323648@163.com (K.L.); kongyiwen0227@163.com (Y.K.); hxl014@126.com (X.H.)
[2] College of Animal Science and Technology, Gansu Agricultural University, Lanzhou 730070, China; gunsb@gsau.edu.cn
[3] Institute of Animal Science and Veterinary Medicine, Hainan Academy of Agricultural Sciences, Haikou 571100, China
[4] College of Animal Science and Technology, Hainan University, Haikou 570228, China
* Correspondence: lxjlongfei@163.com (X.L.); yutong@henau.edu.cn (T.Y.)

Abstract

Porcine oocytes are susceptible to oxidative stress and mitochondrial dysfunction during in vitro maturation (IVM), which compromises their maturation quality, cryotolerance, and subsequent developmental competence. Therefore, improving the efficiency of IVM and cryopreservation is of great significance for the conservation of livestock genetic resources. In human medicine, oocyte IVM and vitrification can promote the development of assisted reproductive technology. In this study, we supplemented the maturation medium with various concentrations (0, 20, 30, 40, and 50 μM) of chlorogenic acid (CGA) to evaluate its effects on the porcine oocyte maturation rate. Transcriptome sequencing (RNA-seq) of pooled oocytes based on Smart-seq2 was performed to elucidate the key molecular pathways associated with CGA during porcine oocyte IVM. Compared with the control group, treatment with 30 μM CGA significantly improved the maturation rate (control group 64.83% ± 1.51% vs. 30 μM CGA treat group 77.86% ± 2.00%, $p < 0.05$). However, the Cumulus Expansion Index was not significantly altered by any of the CGA treatments ($p > 0.05$). RNA-seq identified 167 differentially expressed genes (DEGs) between the two groups. Kyoto Encyclopedia of Genes and Genomes enrichment analysis revealed that these DEGs were predominantly enriched in ribosome, oxidative phosphorylation (OXPHOS), and thermogenesis. Gene Ontology functional enrichment showed that the upregulated genes were mainly associated with translation, ribosome, mitochondrial respiratory chain complex I assembly, and other related terms. Protein–protein interaction network analysis indicated that the DEGs were primarily enriched for genes involved in the composition of cytosolic ribosomal subunits (*RPS27A*, *RPL13A*, *RPL26*, *RPL9*, and *RPS13*). Real-time quantitative PCR validation of four randomly selected DEGs yielded expression trends consistent with the RNA-seq data. Furthermore, compared with the control group, supplementation of the IVM medium with 30 μM CGA significantly increased intracellular glutathione (GSH) levels ($p < 0.05$), mitochondrial membrane potential ($p < 0.05$), and MitoTracker fluorescence intensity in fresh oocytes ($p < 0.01$). In vitrified-warmed oocytes, 30 μM CGA treatment similarly elevated GSH levels ($p < 0.01$) and did not significantly alter ROS levels ($p > 0.05$), while significantly improving the short-term post-warming survival rate (control group 60.79% ± 3.92% vs. 30 μM CGA treat group 82.15% ± 5.22%,

Check for updates

Academic Editor: Ana B Rodríguez Moratinos

Received: 23 September 2026
Revised: 9 November 2026
Accepted: 11 November 2026
Published: 16 November 2026

Copyright: © 2026 by the authors. Licensee MDPI, Basel, Switzerland. This article is an open access article distributed under the terms and conditions of the Creative Commons Attribution (CC BY) license.

$p < 0.05$). However, in freshly matured oocytes, CGA did not significantly affect intracellular ROS levels, early apoptosis, or the subsequent developmental competence of embryos derived from in vitro fertilization ($p > 0.05$). Collectively, these findings demonstrate that 30 μM CGA improves oocyte maturation efficiency, increases intracellular GSH levels, and enhances mitochondrial status in porcine oocytes, and short-term post-warming survival of vitrified porcine oocytes. These beneficial effects are associated with changes in the expression of genes related to ribosome and OXPHOS pathways. This study provides a reference basis for optimizing the IVM and warrants future investigation into vitrification preservation for porcine oocytes.

Keywords: porcine oocytes; chlorogenic acid; in vitro maturation; oxidative stress; embryonic development

1. Introduction

Mammalian oocyte maturation and vitrification are two critical procedures in modern reproductive biotechnology, holding substantial importance for the conservation of genetic resources, propagation of elite germplasm, and protection of endangered species. Oocyte maturation in mammals is a prerequisite for successful fertilization and early embryonic development. Moreover, the availability of numerous mature oocytes provides essential biological materials for in vitro embryo production (IVP) and somatic cell nuclear transfer (SCNT) in livestock [1,2]. Vitrification, currently one of the most promising techniques for oocyte preservation, not only circumvents the potential risks of disease transmission associated with in vivo conservation, but also enables long term storage of genetic resources, facilitates safe international exchange and efficient utilization of germplasm, and, to a certain extent, replaces the costly transportation of live large animals, thereby reducing costs and enhancing biosecurity [3,4].

The pig is a major livestock species that contributes significantly to the national economy. Moreover, as a valuable large animal model for biomedical research, the availability of large numbers of its oocytes provides substantial resources for human organ transplantation and investigations of related diseases. Consequently, improving the maturation rate and embryo production efficiency of porcine oocytes is of critical importance. Oocyte maturation proceeds through a first meiotic arrest, known as the germinal vesicle (GV) stage. Germinal vesicle breakdown and the extrusion of the first polar body mark the completion of the first meiotic division, after which the oocyte enters the second meiotic division and arrests at metaphase II (MII) until fertilization or ovulation [5]. However, during in vitro maturation (IVM), oocytes are exposed to non-physiological conditions, leading to excessive accumulation of reactive oxygen species (ROS) and subsequent oxidative stress, which can induce lipid peroxidation of cellular membranes, protein conformational alterations, and DNA damage, thereby significantly compromising oocyte quality and subsequent developmental competence [6]. Furthermore, oocyte quality not only determines its ability to undergo in vitro fertilization (IVF), but also directly influences its tolerance to low temperature stress. During vitrification, oocytes are subjected to multiple stressors, including exposure to high concentrations of cryoprotectants, drastic osmotic changes, and ultra-rapid temperature fluctuations [7,8], all of which further exacerbate oxidative damage, cytoskeletal disruption, and mitochondrial dysfunction, ultimately impairing oocyte survival and developmental capacity. Therefore, the regulation of oxidative stress during maturation is considered a critical determinant for enhancing both the efficiency of oocyte IVM and the success of vitrification.

Previous studies have demonstrated that the application of antioxidants, such as melatonin [9], resveratrol [10], taurine [11], and β-nicotinamide mononucleotide [12], can enhance the maturation efficiency of porcine oocytes and improve their subsequent embryonic developmental potential. In addition to the aforementioned compounds, phenolic acids derived from natural herbs, particularly chlorogenic acid (CGA), are widely present in various agricultural products. The primary forms include ester compounds such as caffeoylquinic acid, dicaffeoylquinic acid, feruloylquinic acid, and caffeoylferuloylquinic acid, among others [13,14]. Owing to its ability to scavenge excess intracellular ROS, reduce oxidative substances, and counteract apoptosis, CGA has been extensively applied in diverse research contexts, including the repair of hepatocyte injury in mice [15–17], intestinal stem cell regeneration in mice [18], amelioration of lipid metabolism disorders in rats and mice [19–21], diabetes treatment [22], and alleviation of heat stress-induced damage in porcine Sertoli cells [23]. These findings collectively position CGA as a promising candidate for providing valuable therapeutic targets in human disease treatment and the advancement of regenerative medicine. Concurrently, considerable research has been conducted on the effects of CGA on mammalian gametes and embryonic development. For instance, supplementation of CGA during IVM and vitrification of sheep oocytes has been shown to reduce ROS levels, elevate glutathione (GSH) content and mitochondrial membrane potential (MMP), and improve maturation rates as well as post-vitrification cleavage and blastocyst rates [24]. In the context of semen preservation, CGA improves sperm motility and plasma membrane integrity in boars, rams, and humans [25–27]. Moreover, CGA alleviates heat stress induced damage during porcine oocyte maturation, thereby increasing blastocyst formation under heat stress conditions [28]. Supplementation with 50 μM CGA during porcine oocyte maturation suppresses apoptosis and enhances the developmental competence of electroporated porcine embryos [29], and its addition to the culture medium of SCNT embryos from Vietnamese indigenous Ban pigs similarly improves embryo quality [30]. Although the previous studies have thoroughly demonstrated the positive effects of CGA on oocyte maturation and embryonic development, most of these findings remain confined to phenotypic assessments, such as maturation rate, parthenogenetic blastocyst rate, and blastocyst cell numbers [31,32]. Nevertheless, the molecular regulatory networks and underlying mechanisms through which CGA orchestrates porcine oocyte maturation have yet to be fully elucidated, and its application in the vitrification of porcine oocytes has not been reported.

The present study employed porcine oocytes as a research model to evaluate the effects of CGA on oocyte maturation rates. Furthermore, leveraging RNA sequencing (RNA-seq), we aimed to decipher, at the global transcriptional level, the key molecular players and signaling pathways through which CGA orchestrates porcine oocyte maturation. This work is expected to fill the aforementioned mechanistic void and provide novel theoretical foundations for optimizing the IVM system and vitrification preservation of porcine oocytes.

2. Materials and Methods

2.1. Materials and Reagents

All reagents used in the present study were purchased from Sigma-Aldrich Co. (Alcobendas, Madrid, Spain), unless otherwise stated.

2.2. Preparation of Media and Solutions

To prepare the 5 mM stock solution, 1.7716 mg of CGA (HY-N0055, MCE, Shanghai, China) was dissolved in 1 mL of double-distilled water (ddH_2O). The stock solution was sterilized by filtration through a 0.22 μm membrane filter and stored at −80 °C until use.

Prior to each experiment, the stock solution was diluted with porcine IVM medium to final working concentrations of 0, 20, 30, 40, and 50 μM.

2.3. Oocyte Collection and IVM

Porcine ovaries were collected from a local slaughterhouse (located in Zhengzhou, China) and transported to the laboratory in physiological saline at 38 °C within 2 h, where they were washed thoroughly. Follicular fluid was aspirated from follicles of 2–6 mm in diameter using a 10 mL syringe. Cumulus–oocyte complexes (COCs) with at least three layers of compact cumulus cells were selected under a stereomicroscope and subjected to IVM. The COCs were cultured in M199 medium supplemented with 10 ng/mL epidermal growth factor (EGF), 10 ng/mL follicle stimulating hormone (FSH), 0.5 μg/mL luteinizing hormone (LH), 20 ng/mL insulin-like growth factor 1, 0.57 mM cysteine, 0.91 mM sodium pyruvate, 0.35 mM glucose, 0.1% polyvinyl alcohol, and 1% antibiotic–antibodies. The maturation was performed at 38.5 °C in a humidified atmosphere of 5% CO_2 for 42–44 h. Oocytes were incubated with 0.5% (*w*/*v*) hyaluronidase dissolved in maturation medium at 38.5 °C in a 5% CO_2 incubator for 3–5 min to remove cumulus cells. The oocytes were then examined under a stereomicroscope, and the number of oocytes that had extruded the first polar body was recorded. In this study, MII oocytes matured in vitro from fresh GV-stage oocytes were used as the control group, and MII oocytes obtained from IVM supplemented with 20, 30, 40, and 50 μM CGA were used as the treatment groups. The oocyte maturation rate was calculated as the number of oocytes that had extruded the first polar body divided by the total number of oocytes examined × 100%.

2.4. Measurement of Cumulus Expansion Index

Following in IVM (for 42–44 h), to quantify the expansion status of cumulus–oocyte complexes (COCs), morphological evaluation was performed using the Cumulus Expansion Index (CEI) based on previous studies [33,34]. First, based on the extent of cumulus cell layer migration, the expansion status of COCs was graded into five levels: Grade 0, no signs of cumulus expansion; Grade 1, expansion restricted to the outermost 1–2 layers of cumulus cells; Grade 2, obvious radial extension of the outer cumulus cells, causing the overall COC structure to become loose; Grade 3, full expansion of cumulus cells in all regions except the corona radiata; and Grade 4, complete expansion of all cumulus cells, including the corona radiata. The CEI was calculated using the following formula: CEI = [(Number of Grade 0 oocytes × 0) + (Number of Grade 1 oocytes × 1) + (Number of Grade 2 oocytes × 2) + (Number of Grade 3 oocytes × 3) + (Number of Grade 4 oocytes × 4)]/Total number of oocytes.

2.5. RNA-Seq and Analysis

The 30 μM CGA concentration was selected based on our preliminary experiments, in which 30 μM CGA supplementation during IVM significantly improved the oocyte maturation rate without obvious cytotoxicity. This concentration was therefore used for transcriptome analysis. Oocytes from the control and 30 μM CGA-treated groups were harvested in triplicate, with 17 oocytes per replicate. Pooled samples, rather than individual oocytes, were treated as the independent experimental units for differential expression analysis. After rinsing at least three times with phosphate-buffered saline with polyvinyl alcohol (PBS-PVA), the oocytes were transferred into lysis buffer (BGI, Wuhan, China) for complete disruption to release total RNA, and the lysates were kept at −80 °C until processing. Amplified products were assessed for quality: those exhibiting a major peak between 800 and 2000 bp and a concentration above 0.2 ng/μL were deemed eligible; samples with a major peak below 800 bp or displaying sharp peaks beyond 800 bp were

discarded. In the current study, the measured concentrations fell within 33.54–43.42 ng/μL, and the major peak in the amplified products was consistently observed at 800–2000 bp, thus satisfying the prerequisites for library construction. Subsequently, poly(A)-tailed mRNA was captured using Oligo (dT) conjugated magnetic beads. The captured RNA was fragmented, and first strand cDNA was synthesized with random N6 primers, followed by second-strand synthesis to generate double-stranded cDNA. The double-stranded products were then end-repaired, 5′-phosphorylated, and subjected to A-tailing at the 3′ end, after which adapters bearing a 3′ T-overhang were ligated. The ligation products were amplified by PCR and converted into single-stranded DNA, which was subsequently circularized via bridge primers to obtain single-stranded circular DNA libraries. Following quality verification, the qualified libraries were processed for sequencing.

RNA-seq was conducted on the DNBSEQ platform with a PE100 read length. Raw reads were processed using SOAPnuke software (v2.1.9) [35] for quality control to remove low quality reads, adapter contaminated reads, and reads containing unknown bases (N) at a proportion exceeding 0.1%. The resulting clean reads were aligned to the porcine reference genome (Sscrofa11.1) using HISAT (v2.2.1) [36], and the alignment rates and read distributions across the reference genome were assessed. Subsequently, clean reads were mapped to the reference gene set using Bowtie (v2.3.4) [37], and gene expression levels were quantified using RSEM (v1.3.1) [38], which generated both raw read counts and Transcripts Per Million (TPM) values. For gene expression quantification, TPM was used as the primary normalization method. *p*-values were adjusted using the Benjamini–Hochberg method to control the False Discovery Rate (FDR). For differential expression analysis, the raw read counts were used as input for DESeq2 (v1.4.5) to identify differentially expressed genes (DEGs). DESeq2 internally normalized the counts using the median-of-ratios method [39]. Genes with thresholds of $|\log_2 FC| \geq 0.58$ and Q value < 0.05 were considered significantly differentially expressed. For data visualization, the TPM values were used to perform hierarchical clustering and generate expression heatmaps using the pheatmap (v1.0.8) package in R (v4.3.1). Gene Ontology (GO) (http://www.geneontology.org/) and Kyoto Encyclopedia of Genes and Genomes (KEGG) (https://www.kegg.jp/) enrichment analyses were performed using Phyper based on the hypergeometric test, with pathways having a Q value ≤ 0.05 considered significantly enriched. The STRING database (https://cn.string-db.org/) and Cytoscape software (v3.9.1) were employed to construct the protein–protein interaction (PPI) network of the DEGs.

2.6. Measurement of Intracellular ROS and GSH Levels

To assess intracellular ROS and GSH levels, the IVM oocytes were incubated in 100 μL of 10 μM DCFH-DA (S0033S, Beyotime, Shanghai, China) for 20 min, or 10 μM Monochlorobimane (HY-101899, MCE, Shanghai, China) for 30 min at 38.5 °C in a 5% CO_2 incubator. After incubation, the oocytes were washed three times with culture medium. Subsequently, the oocytes were examined under an inverted fluorescence microscope, and the fluorescence intensity of each oocyte was quantified using ImageJ (v1.54). All experiments were performed in triplicate.

2.7. Assessment of MMP and Mitochondrial-Associated Fluorescence in Oocytes

After 42–44 h of maturation, MMP was assessed using JC-1 staining according to the manufacturer's instructions. Briefly, the JC-1 dyes (C2006, Beyotime, Shanghai, China) was diluted with oocyte culture medium and pre-warmed at 38.5 °C in a 5% CO_2 incubator for 20 min. Subsequently, oocytes were incubated in 50 μL of the JC-1 staining solution at 38.5 °C in 5% CO_2 in the dark for 20 min. After incubation, the oocytes were washed three times with 1 × JC-1 washing buffer. Finally, the oocytes were examined under a fluorescence

microscope, and images were captured. The red and green fluorescence intensities of each oocyte were analyzed using ImageJ (v1.54), and the MMP was expressed as the ratio of red to green fluorescence intensity. All experiments were performed in triplicate.

Mitochondrial-associated fluorescence in oocytes was assessed using MitoTracker staining according to the manufacturer's instructions (C1049, Beyotime, Shanghai, China). Briefly, MitoTracker was diluted to 5 μM, and oocytes were transferred into 50 μL droplets of the MitoTracker working solution. The oocytes were then incubated at 38.5 °C in a 5% CO_2 incubator in the dark for 20 min. After incubation, the oocytes were washed three times with culture medium and photographed under a fluorescence microscope. The fluorescence intensity of each oocyte was measured using ImageJ (v1.54) software. All experiments were performed in triplicate.

2.8. Detection of Early Apoptosis in Oocytes

To assess early apoptosis, matured oocytes were transferred into 50 μL droplets of a working solution prepared by mixing 195 μL Annexin V-FITC binding buffer with 5 μL Annexin V-FITC staining solution (C1062S, Beyotime, Shanghai, China) and incubated at room temperature (20–25 °C) incubator in the dark for 20 min. After incubation, the oocytes were washed three times with culture medium and photographed under a fluorescence microscope. All experiments were repeated three times.

2.9. IVF and Embryo Culture

The matured oocytes were placed into fertilization droplets for insemination. A discontinuous Percoll gradient was prepared by adding 1.2 mL of 80% Percoll to a 15 mL centrifuge tube, followed by the slow overlay of 1.2 mL of 40% Percoll. The tube containing both layers was placed vertically in the incubator and pre-equilibrated for 30 min. Fresh semen was gently layered onto the top of the pre-equilibrated Percoll gradient in the 15 mL tube and centrifuged at 300× *g* for 10 min. The supernatant was discarded, and the sperm pellet was transferred to 3 mL of pre-equilibrated HEPES-buffered medium, resuspended by gentle pipetting, and centrifuged again at 400× *g* for 5 min. After removing the supernatant, the sperm pellet was kept for subsequent use. Spermatozoa were added to the fertilization droplets at a final concentration of 1×10^5 sperms/mL. Following co-incubation for 6 h, the presumptive zygotes were transferred to embryo culture medium and cultured further. Cleavage rates were recorded on Day 2, and blastocyst rates were assessed on Day 7. The cleavage rate was calculated as the number of cleaved embryos divided by the total number of oocytes inseminated × 100%, and the blastocyst rate was calculated as the number of blastocysts divided by the number of cleaved embryos × 100%. Notably, only freshly matured oocytes were used for these IVF experiments; vitrified-warmed oocytes were not subjected to IVF in this study.

2.10. Oocyte Vitrification and Warming

In the vitrification experiment, MII oocytes vitrified after IVM in CGA-free maturation medium served as the control group, whereas those vitrified after IVM in maturation medium supplemented with 20, 30, 40, or 50 μM CGA served as the treatment groups. Oocyte vitrification was performed using the Cryotop device (Minvitro, Guangzhou, China). Briefly, mature oocytes were first equilibrated in M199-based equilibration solution (ES) containing 7.5% (*v*/*v*) ethylene glycol (EG), 7.5% (*v*/*v*) dimethyl sulfoxide (DMSO), and 20% (*v*/*v*) fetal bovine serum (FBS) for 5 min. The oocytes were then transferred to M199-based vitrification solution (VS) supplemented with 15% (*v*/*v*) EG, 15% (*v*/*v*) DMSO, 20% (*v*/*v*) FBS, and 0.5 M sucrose for 20–30 s. Immediately thereafter, 10–15 oocytes with a minimal volume of VS (<0.1 μL) were loaded onto the Cryotop device (Minvitro,

Guangzhou, China) and plunged directly into liquid nitrogen. The entire procedure from exposure of oocytes to VS to immersion in liquid nitrogen was completed within 60 s.

After storage in liquid nitrogen for one week, the oocytes were warmed. The Cryotop was removed from liquid nitrogen and immediately immersed in M199 medium containing 0.4 M sucrose and 20% FBS for 2 min. Subsequently, the oocytes were sequentially transferred through M199 media supplemented with 20% FBS and decreasing concentrations of sucrose (0.3, 0.2, and 0.1 M), with 1 min incubation at each step. The oocytes were then placed in M199 medium with 10% FBS for 3 min, followed by three washes in oocyte culture medium. Finally, the warmed oocytes were cultured in an incubator for 2 h to allow recovery. Under a stereomicroscope, oocytes with uniform and refractive cytoplasmic granules, an intact zona pellucida, and a distinct perivitelline space were considered viable. In contrast, oocytes exhibiting a ruptured zona pellucida, shrunken cytoplasm, and an indistinct or absent perivitelline space were classified as non-viable.

2.11. Trypan Blue Stain

After recovery culture for 2 h, oocytes were placed in 0.04% Trypan Blue staining solution (T8070, Solarbio, Beijing, China) and incubated at room temperature for 3–5 min. The oocytes were then washed three times with PBS-PVA. Viable and non-viable oocytes were counted separately under a microscope. Oocytes stained blue were classified as non-viable, whereas unstained oocytes were considered viable. The survival rate was calculated as (number of viable oocytes/total number of oocytes) × 100%. This assessment specifically reflects short-term post-warming survival and membrane integrity, as previously described.

2.12. Real-Time Quantitative Polymerase Chain Reaction (qPCR)

Gene primers were designed using the NCBI database (https://www.ncbi.nlm.nih.gov/) (see Table 1). For sample preparation, MII-stage oocytes collected on the same day were considered as one independent biological replicate. A total of three independent biological replicates ($n = 3$) were included for each experimental group. In each replicate, 20 mature MII-stage oocytes were randomly selected and thoroughly lysed in lysis buffer for total RNA extraction, and the RNA samples were stored at −80 °C until use. Reverse transcription of mRNA to cDNA was performed using the Evo M-MLV RT Mix Kit (AG11728, Accurate Biology, Nanjing, China). To precisely quantify mRNA levels, qRT-PCR was carried out on a C1000 Touch™ Thermal Cycler (Thermo Fisher Scientific, Shanghai, China). The 10 µL reaction mixture contained 1 µL of cDNA template, 5 µL of SYBR Green Master Mix, 0.4 µL each of forward and reverse primers, and 3.2 µL of ddH_2O. The thermal cycling protocol consisted of an initial denaturation at 95 °C for 1 min, followed by 40 cycles of denaturation at 95 °C for 15 s, annealing at 60 °C for 30 s, and extension at 72 °C for 30 s. β-Actin was used as the reference gene, and relative gene expression levels were calculated using the $2^{-\Delta\Delta Ct}$ method.

Table 1. qRT-PCR primer sequences.

Gene Name	GenBank Accession	Sequence (5′-3′)	Length (bp)
β-actin	NM_001444420.1	F: GACCACCTTCAACTCGATCAT R: GATCTCCTTCTGCATCCTGTC	124
YWHAE	XM_021067551.1	F: ATGCAGGGTGATGGTGAAGAG R: GAATTTCCAAGAGGGGTGGGA	138
RPL30	NM_001190178.1	F: CGAAGAGCTTGGCATTGTGG R: ACTCCAGCGACTTTTTCGTC	135

Table 1. *Cont.*

Gene Name	GenBank Accession	Sequence (5′-3′)	Length (bp)
NDUFAB1	XM_005656762.3	F: CGATCCCGAAAAGCTCTCAGT R: GGGCACATTAACTTCTCCGC	144
CHMP3	XM_003354734.4	F: CGGAAGGGGCAAGACGAGTT R: ATGACCATTCATTGACAGCTCT	90

2.13. Statistical Analysis

No oocytes or experimental runs were excluded from the final statistical analysis in an ad hoc manner. In this study, the experimental unit was defined as a batch of oocytes collected from a separate set of ovaries on a different experimental day. For the IVM experiment, oocytes were randomly assigned to the control and four treatment groups within each replicate. The maturation rate was calculated independently for each batch, and statistical analysis was based on six independent biological replicates ($n = 6$), rather than individual oocytes. For the evaluation of oxidative stress and mitochondrial status (fluorescence staining), oocytes from three independent biological replicates ($n = 3$) were analyzed, with each batch serving as one experimental unit. For the IVF experiment, the experimental unit was defined as one complete in vitro embryo production procedure performed on a separate batch of freshly matured oocytes. Cleavage and blastocyst rates were calculated for each independent run, and data were analyzed based on four ($n = 4$) and three ($n = 3$) independent replicates, respectively. In all experiments, the total number of oocytes analyzed (N) is reported alongside the number of replicates (n) to ensure statistical rigor.

All data in this study were analyzed using GraphPad Prism 9.50 software. For data that met the normal distribution, one-way analysis of variance (ANOVA) followed by Tukey's multiple comparisons test was used for post hoc comparisons. For data that did not meet the normal distribution, the Kruskal–Wallis non-parametric test was used. Comparisons between two groups were performed using independent samples Student's t-test. No multiple-testing correction was required for qPCR, as a single pairwise comparison was made for each gene. Data were expressed as mean ± SEM. Fluorescence images were analyzed using ImageJ (v1.54) software, and qRT-PCR results were calculated using the $2^{-\Delta\Delta Ct}$ method. Statistical significance is indicated as follows: ns, not significant ($p > 0.05$); * $p < 0.05$; ** $p < 0.01$.

3. Results and Analysis

3.1. CGA Promotes Porcine Oocyte Maturation In Vitro

To investigate whether low concentrations of CGA could improve the efficiency of porcine oocyte IVM and to explore the underlying mechanisms, an experimental design was established as illustrated in Figure 1A. Different concentrations of CGA (0, 20, 30, 40, and 50 μM) were supplemented into the porcine oocyte IVM medium to evaluate their effects on cumulus cell expansion and oocyte maturation rates. Representative images of cumulus expansion are presented in Figure 1B. Quantitative analysis using the CEI revealed no statistically significant differences among the groups ($p > 0.05$, Figure 1C). Oocytes that had extruded the first polar body were considered mature (Figure 1D), and the maturation rates were subsequently calculated. The results showed that the maturation rates in all CGA treated groups were higher than those in the control group. Notably, the maturation rate in the 30 μM CGA group (77.86% ± 2.00%, $N = 187$, $n = 6$) was significantly higher than that in the control group (64.83% ± 1.51%, $N = 157$, $n = 6$, $p < 0.05$). Although the maturation rates in the 20 μM (76.03% ± 3.40%, $N = 172$, $n = 6$), 40 μM (76.55% ± 2.71%, $N = 182$,

$n = 6$), and 50 μM (66.21% ± 4.79%, $N = 182$, $n = 6$) groups were also increased, they did not differ significantly from the control group ($p > 0.05$; Table 2). Based on these findings, 30 μM was selected as the most promising concentration for subsequent experiments.

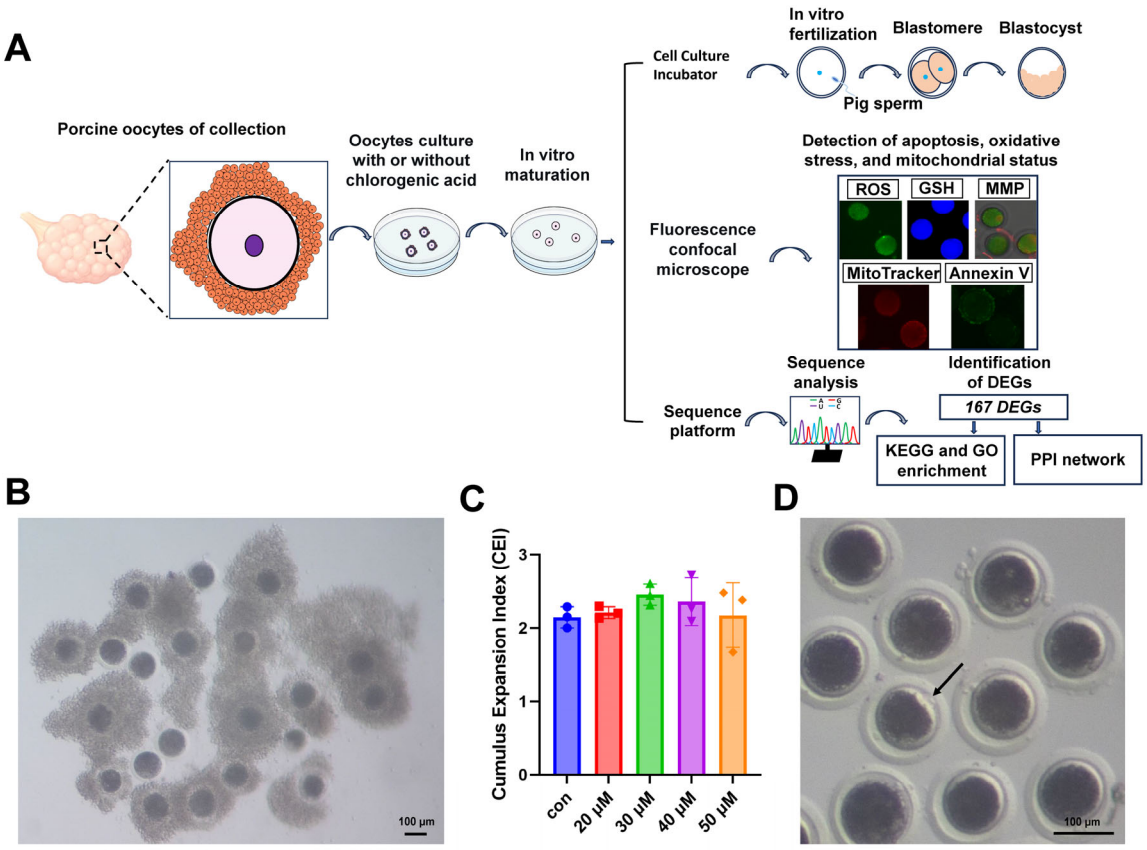


Figure 1. Effects of CGA on cumulus expansion and IVM of porcine oocytes. (**A**) Experimental design workflow. ROS, reactive oxygen species; GSH, glutathione; MMP, mitochondrial membrane potential; DEGs, differentially expressed genes; KEGG, Kyoto Encyclopedia of Genes and Genomes; GO, Gene Ontology; PPI, protein-protein interaction. (**B**) Representative images of cumulus expansion in porcine COCs (scale bar = 100 μm). (**C**) Quantitative analysis of the CEI. Data are presented as mean ± SEM from three independent biological replicates ($n = 3$), with 11–20 COCs analyzed per replicate. Con, control group; 20 μM–50 μM, chlorogenic acid treat group. No statistically significant differences were observed among the groups ($p > 0.05$). (**D**) Representative images of matured oocytes, with arrows indicating the first polar body (scale bar = 100 μm).

Table 2. Effects of Different Concentrations of CGA on Porcine Oocyte Maturation Rate.

Group	No. of Oocytes	No. of Mature Oocytes	No. of Immature Oocytes	Maturation Rate
Con	157	102	55	64.83 ± 1.51% ^{b}
CGA-20 μM	172	131	41	76.03 ± 3.40% ^{ab}
CGA-30 μM	187	147	40	77.86 ± 2.00% ^{a}
CGA-40 μM	182	139	43	76.55 ± 2.71% ^{ab}
CGA-50 μM	182	121	61	66.21 ± 4.79% ^{ab}

Note: Data are expressed as mean ± SEM. Within the same column, values with different superscript letters differ significantly ($p < 0.05$), whereas those with the same superscript letter do not ($p > 0.05$). Statistical comparisons were performed on replicate-level percentages ($n = 6$), with 16–41 oocytes per replicate.

3.2. Effects of CGA Supplementation on the Transcriptome Profiles of Porcine Oocytes

To gain further insight into how CGA improves the porcine oocyte maturation rate and to elucidate its functional mechanisms, RNA-seq was performed on mature oocytes from the control group and the 30 μM CGA supplemented group. The sequencing run generated 242.87 M raw reads, which yielded 188.73 M clean reads (corresponding to 37.75 Gb of clean bases) after quality filtering, with mean Q20 and Q30 values of 98.93% and 96.96%, respectively. On average, 97.72% (range: 97.60–97.79%) of the clean reads were mapped to the reference genome, with 92.84% (range: 92.24–93.27%) of the reads uniquely mapped (Table S1). A total of 17, 173 genes were quantified across all samples. Sample correlation analysis showed that all inter sample correlations exceeded 0.97 (Figure 2A). Principal component analysis (PCA) revealed that biological replicates within each group clustered closely together, while the control and CGA-treated groups were clearly separated (Figure 2B), indicating distinct transcriptional profiles between the two groups. Subsequently, differential expression analysis was performed to identify DEGs between the two groups. A total of 167 DEGs were identified, including 138 significantly upregulated and 29 significantly downregulated genes (Table S2, Figure 2C). Hierarchical clustering analysis of all DEGs was performed and visualized, yielding results consistent with the PCA pattern and demonstrating that CGA treatment altered the expression patterns of the majority of genes (Figure 2D).

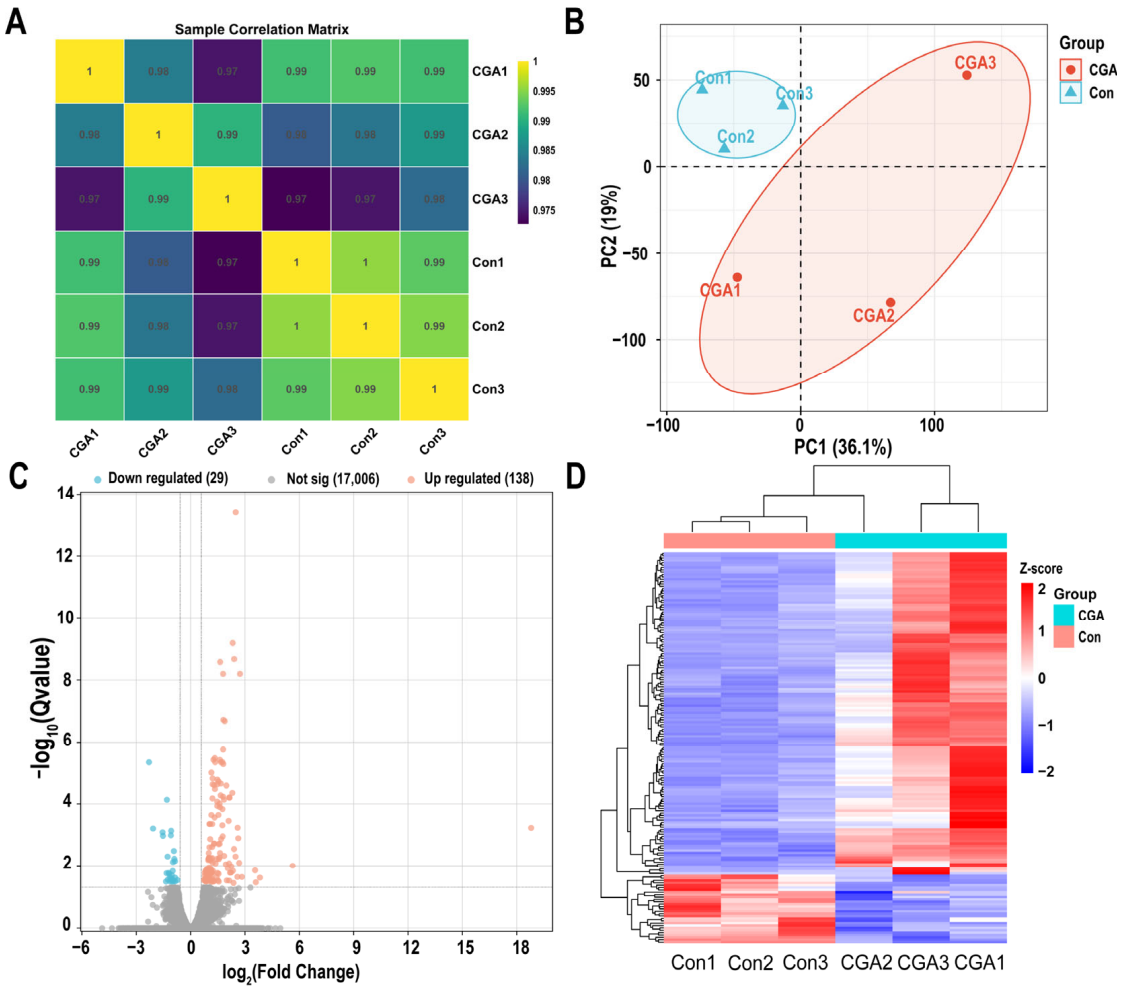


Figure 2. Sample correlation and DEGs analysis. (**A**) sample correlation heatmap displaying the correlation coefficients among all samples. The heatmap displays the Pearson correlation coefficients of gene expression levels between all samples based on transcripts per million (TPM) values; (**B**) PCA

plot showing the separation between the control and CGA-treated groups, the dotted lines represent indicate the zero axes; (**C**) volcano plot of DEGs between the control and CGA-treated groups; (**D**) hierarchical clustering heatmap of DEGs illustrating their expression patterns in the control and CGA-treated groups. The color scale represents the row Z-score of TPM values.

3.3. Enrichment Analysis and Validation of DEGs

To further elucidate the biological functions of the DEGs, KEGG enrichment analysis was performed. The results revealed that the DEGs were predominantly enriched in ribosome, oxidative phosphorylation (OXPHOS), thermogenesis (Table S3, Figure 3A). To evaluate the robustness of our enrichment analysis, DEGs were reidentified using a more stringent threshold ($|\log_2 FC| \geq 1.0$, $Q < 0.05$). Although the total number of DEGs decreased to 135 (Table S4), KEGG enrichment analysis still identified the ribosome and OXPHOS pathways as the significantly enriched terms (Figure S1). GO functional enrichment analysis was conducted on the upregulated genes across three categories: biological process (BP), cellular component (CC), and molecular function (MF). The BP terms were mainly enriched in cytoplasmic translation, mitochondrial respiratory chain complex I assembly, and regulation of translation. The CC terms were predominantly associated with cytosolic ribosome, mitochondrion, cytoskeleton, and mitochondrial inner membrane. The MF terms were primarily enriched in RNA binding, mRNA 5′-UTR binding, and NADH dehydrogenase activity (Table S5, Figure 3B). Given that both GO and KEGG enrichment analyses converged on pathways related to ribosomal composition and mitochondrial OXPHOS, hierarchical clustering analysis was performed to further delineate the distribution patterns of DEGs within these pathways. The results demonstrated that, compared with the control group, several representative DEGs in the ribosome pathway (e.g., *RPS26*, *RPL23A*, *RPS23*, *RPS27*, *RPL2*) and the OXPHOS pathway (e.g., *NDUFS8*, *NDUFB3*, *NDUFA13*, *NDUFAB1*, and *NDUFS6*) were significantly upregulated in the CGA-treated group (Figure 3C,D). This transcriptional profile is associated with the regulation of ribosomal components and mitochondrial respiratory chain genes. Subsequently, PPI network analysis was conducted to identify highly connected hub genes based on network topology. The PPI network highlighted several genes involved in the composition of cytosolic ribosomal subunits, including *RPS27A*, *RPL26*, *RPL9*, *RPL13A*, and *RPS13* (Figure 3E). However, it should be noted that high network connectivity indicates potential interactions based on existing databases, which does not directly establish their functional centrality in CGA action. To validate the reliability of the transcriptomic data, four DEGs were randomly selected for qPCR validation. The qPCR results showed expression trends consistent with the RNA-seq data (Figure 3F,G), confirming the robustness of the sequencing results.

3.4. CGA Enhances Intracellular GSH Levels and Modulates Mitochondrial Status

During IVM, ROS tend to accumulate due to the discrepancy between in vivo and in vitro environments, which may adversely affect subsequent developmental competence. RNA-seq revealed that the DEGs were mainly enriched in OXPHOS and ribosome pathways. Therefore, we investigated whether CGA could enhance the antioxidant capacity and improve mitochondrial function during porcine oocyte IVM. The intracellular redox status was first assessed by measuring ROS and GSH levels. Compared with the control group, supplementation with 30 μM CGA did not significantly alter intracellular ROS levels (Figure 4A,B, $p > 0.05$), but significantly increased GSH levels (Figure 4C,D, $p < 0.05$). To further clarify the impact of CGA on mitochondrial status during IVM, JC-1 and MitoTracker stain were performed. The results showed that treatment with 30 μM CGA significantly enhanced MitoTracker fluorescence intensity (Figure 4E,F, $p < 0.01$) and markedly increased MMP (Figure 4G,H, $p < 0.05$), indicating that 30 μM CGA supplementation during porcine oocyte IVM could significantly improve mitochondrial status. Furthermore, mining of the

transcriptomic data revealed that the mRNA expression levels of mitochondrial function-related genes, including *NDUFS8*, *NDUFB3*, and *NDUFA13*, were significantly higher in the CGA group than in the control group (Figure 4I–K, $p < 0.01$).

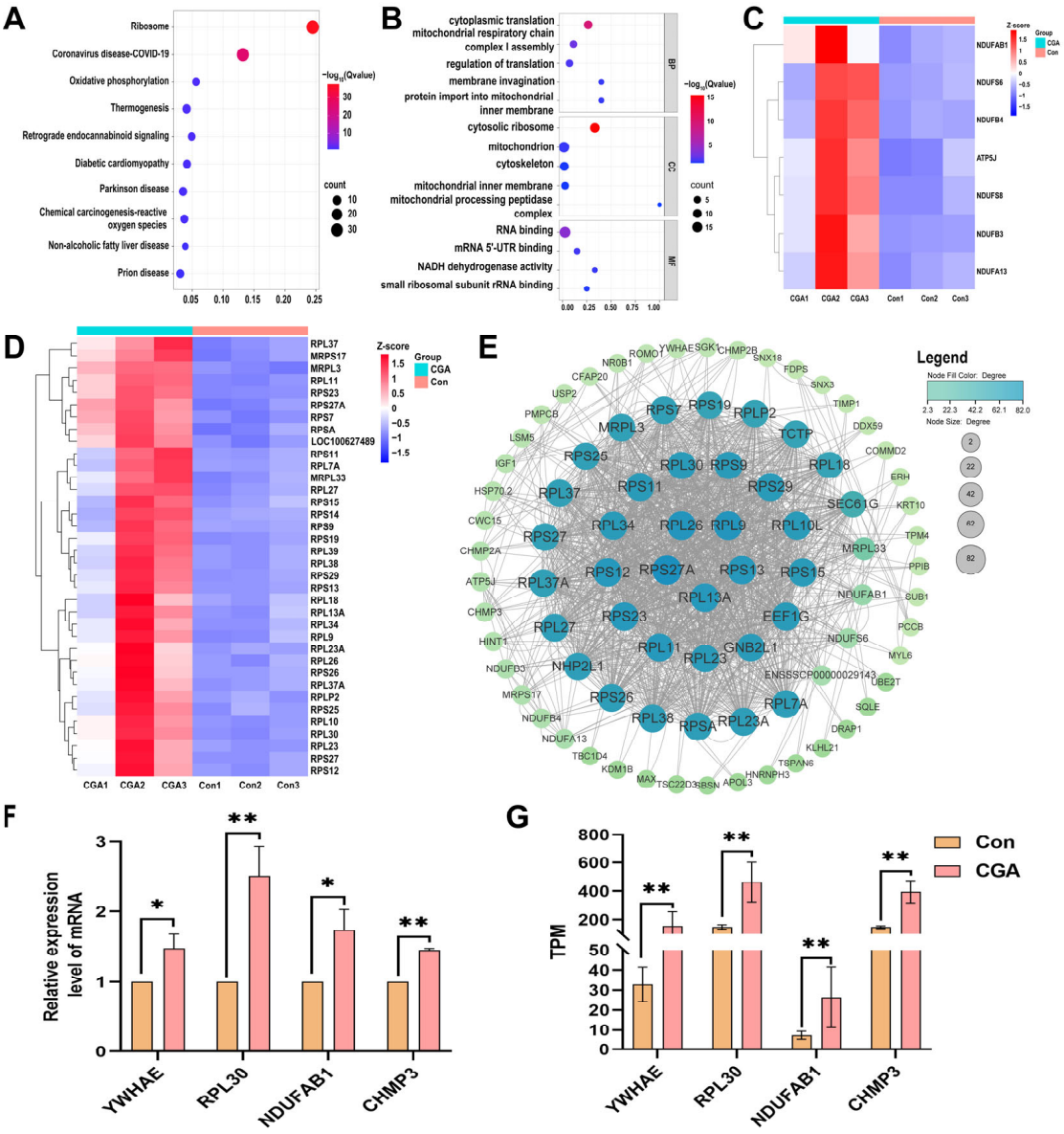


Figure 3. Enrichment analysis and validation of differentially expressed genes. (**A**) Enrichment scatter plots of KEGG enrichment analysis of DEGs; (**B**) scatter plot of GO functional enrichment analysis for upregulated DEGs; (**C**,**D**) clustering heatmap of DEGs involved in the oxidative phosphorylation (OXPHOS) (**C**) and ribosome (**D**) pathways. The color scale represents the row Z-score of TPM values; (**E**) PPI network of DEGs; (**F**,**G**) real-time quantitative polymerase chain reaction validation and TPM expression levels of DEGs, $n = 3$; data are expressed as mean ± SEM, where * $p < 0.05$ indicates a significant difference and ** $p < 0.01$ indicates an extremely significant difference.

3.5. Effects of CGA on Early Apoptosis and Embryonic Development in Porcine Oocytes

To investigate whether CGA could alleviate early apoptosis in porcine oocytes, Annexin-V staining was performed on freshly matured oocytes. The results showed that supplementation with 30 μM CGA did not significantly reduce the early apoptosis rate in oocytes compared with the control group ($p > 0.05$, Figure 5A,B). To further investigate whether supplementation of the oocyte maturation medium with 30 μM CGA could improve embryonic development, freshly matured oocytes from the control and 30 μM CGA-supplemented

groups were subjected to IVF. The results showed that, compared with the control group, the CGA-supplemented group exhibited no significant differences in either cleavage rate (control: 46.36% ± 2.50%, $N = 121$, $n = 4$ vs. CGA-supplemented group 45.30% ± 3.47%, $N = 119$, $n = 4$) or blastocyst rate (control: 11.86% ± 2.24%, $N = 56$, $n = 3$ vs. CGA-supplemented: 11.05% ± 3.68%, $N = 54$, $n = 3$) following IVF (Figure 5C–E, $p > 0.05$).

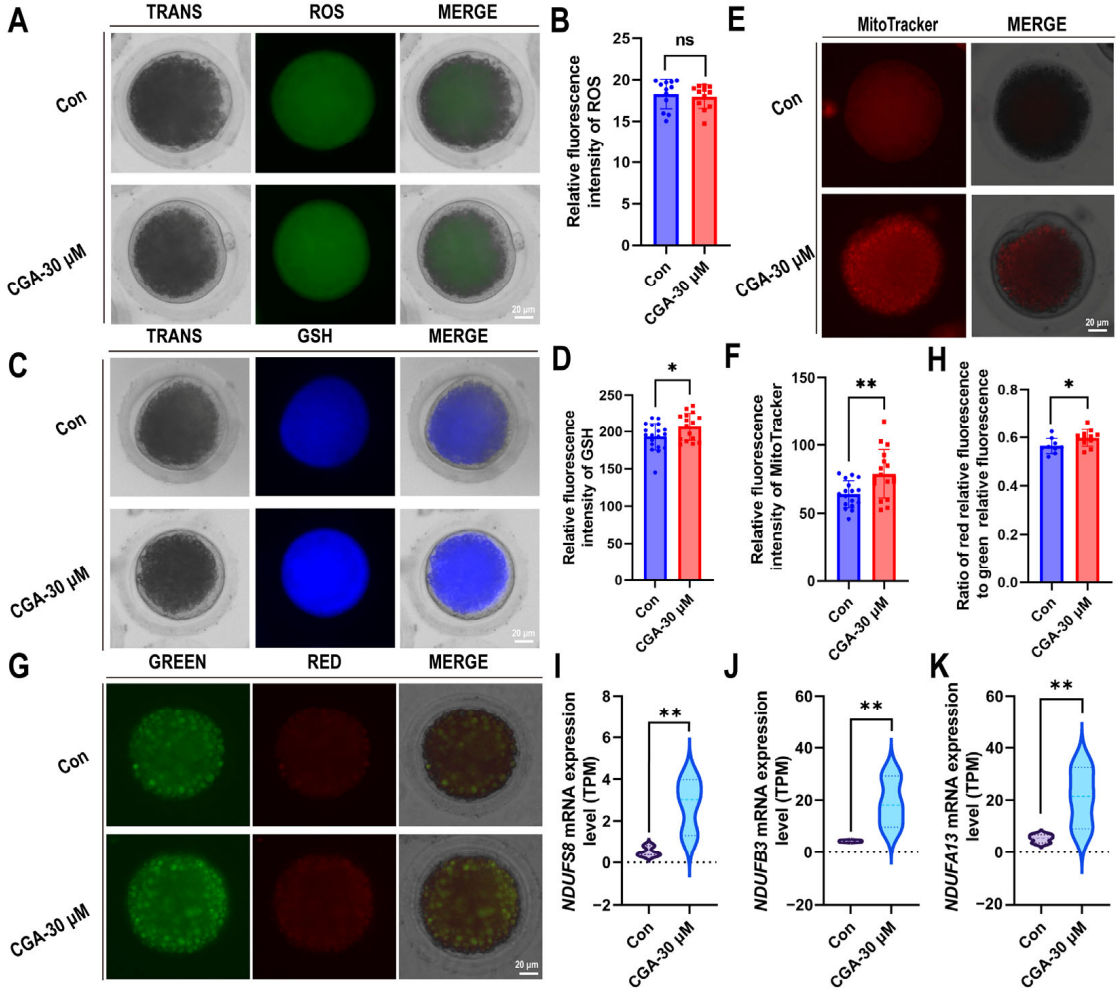


Figure 4. CGA supplementation improved intracellular GSH levels and enhanced mitochondrial status in oocytes. (**A**) Fluorescence images showing intracellular ROS levels detected using DCFH-DA staining (scale bar = 20 μm); (**B**) quantitative analysis of ROS fluorescence intensity (14–20 oocytes per group, $n = 3$); (**C**) fluorescence images of intracellular GSH levels following monochlorobimane staining (scale bar = 20 μm); (**D**) quantification of GSH fluorescence intensity (13–22 oocytes per group, $n = 3$); (**E**) fluorescence images of MitoTracker staining (scale bar = 20 μm); (**F**) statistical analysis of MitoTracker fluorescence intensity (12–17 oocytes per group, $n = 3$); (**G**) representative images of MMP assessed by JC-1 staining (scale bar = 20 μm); (**H**) quantitative measurement of JC-1 fluorescence intensity (9–20 oocytes per group, $n = 3$); (**I**–**K**) TPM of OXPHOS related genes. Data are expressed as mean ± SEM. *, $p < 0.05$; **, $p < 0.01$, ns, not significant $p > 0.05$.

3.6. Effect of CGA on Vitrification Efficiency of Porcine Oocytes

To further determine whether the addition of various concentrations of CGA to the porcine oocyte maturation medium could enhance their cryotolerance, oocytes treated with different concentrations of CGA were subjected to vitrification. Post-vitrification survival was primarily evaluated by morphological observation, with Trypan blue staining used as an auxiliary verification. The results are presented in Table 3. With increasing concentrations of CGA, the oocyte survival rate gradually increased, reaching a peak at

30 μM (82.15% ± 5.22%, $N = 65$, $n = 4$), which was significantly higher than that of the control group (60.79% ± 3.92%, $N = 59$, $n = 4$, $p < 0.05$). Although the survival rates at 20 μM (76.74% ± 8.40%, $N = 63$, $n = 4$) and 40 μM (68.83% ± 3.64%, $N = 75$, $n = 4$) showed an increasing trend, they did not differ significantly from the control ($p > 0.05$). At 50 μM, the survival rate (60.34% ± 2.42%, $N = 73$, $n = 4$) fell below the control level; however, this difference was not statistically significant ($p > 0.05$). To further investigate whether CGA could mitigate oxidative stress in vitrified-warmed porcine oocytes, oocytes from the 30 μM CGA-supplemented group and the control group were subjected to DCFH-DA and Monochlorobimane staining after vitrification and warming. The results showed that, although 30 μM CGA did not significantly reduce ROS levels in vitrified porcine oocytes compared with the control group (Figure 6C,D, $p > 0.05$), it significantly elevated GSH levels (Figure 6E,F, $p < 0.01$).

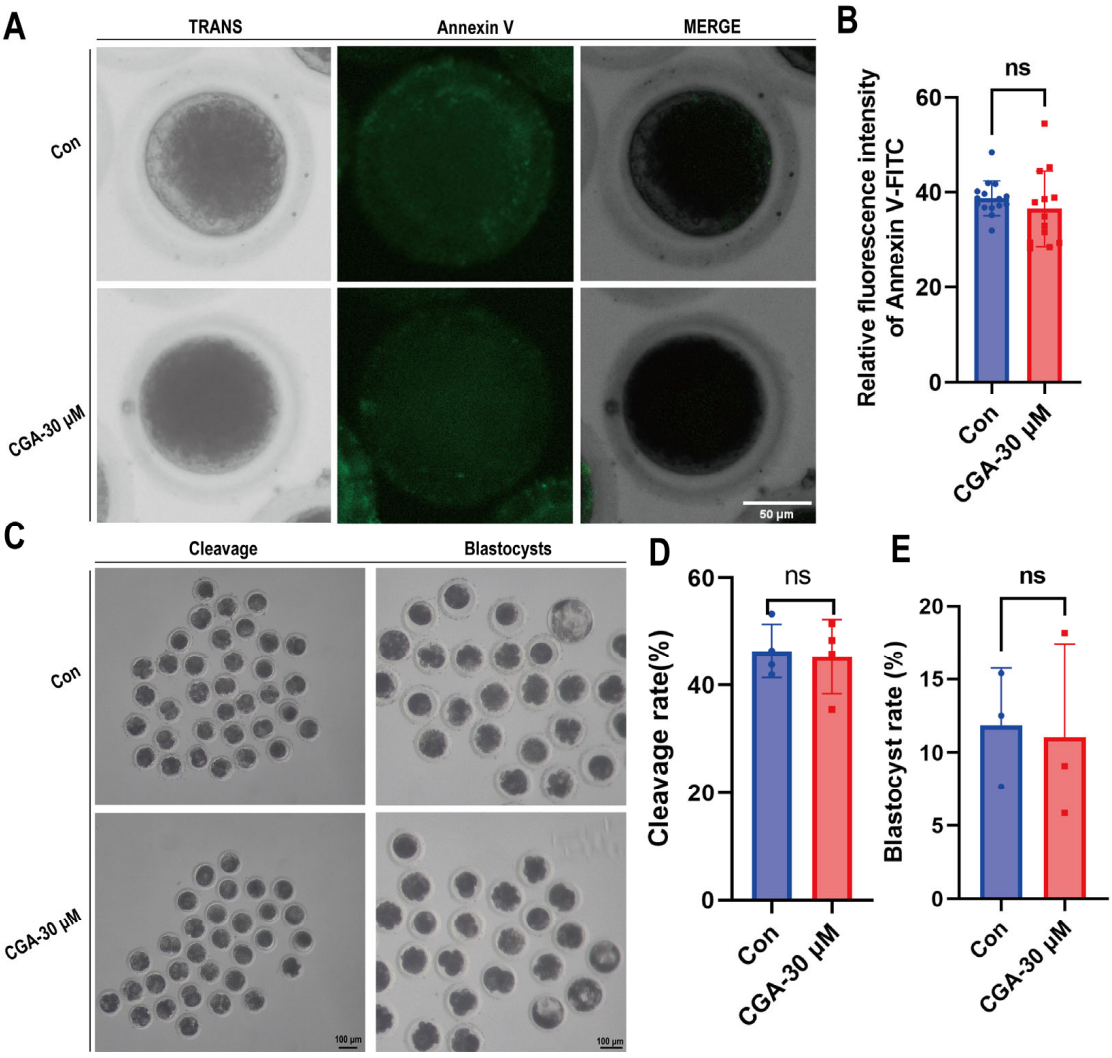


Figure 5. Effects of CGA on early apoptosis and embryonic development of porcine oocytes. (**A**) Representative fluorescence images showing intracellular apoptosis levels detected by Annexin-V staining (scale bar = 50 μm); (**B**) quantitative analysis of Annexin-V fluorescence intensity (13–20 oocytes per group, $n = 3$); (**C**) representative images of cleavage and blastocyst stages following IVF (scale bar = 100 μm). IVF, in vitro fertilization; (**D**) statistical analysis of IVF cleavage rates, data are from four independent biological replicates ($n = 4$), with 24–33 oocytes per replicate per group. (**E**) Statistical analysis of IVF blastocyst rates. Data are from three independent biological replicated ($n = 3$), with 11–17 cleavage oocytes per replicate per group. Data are expressed as mean ± SEM, ns, not significant $p > 0.05$.

Table 3. Effects of Different Concentrations of CGA on the Vitrification Survival Rate of Porcine Oocytes.

Group	No. of Oocytes	No. of Surviving Oocytes	No. of Death Oocytes	Surviving Rate
Con	59	36	23	60.79 ± 3.92% ^{b}
CGA-20 μM	63	51	12	76.74 ± 8.40% ^{ab}
CGA-30 μM	65	53	12	82.15 ± 5.22% ^{a}
CGA-40 μM	75	52	23	68.83 ± 3.64 ^{ab}
CGA-50 μM	73	44	29	60.34 ± 2.42% ^{ab}

Note: Within the same column, different superscript letters indicate significant differences ($p < 0.05$), whereas the same superscript letter indicates no significant difference ($p > 0.05$). Statistical comparisons were performed on replicate-level percentages ($n = 4$), with 8–25 oocytes analyzed per group.

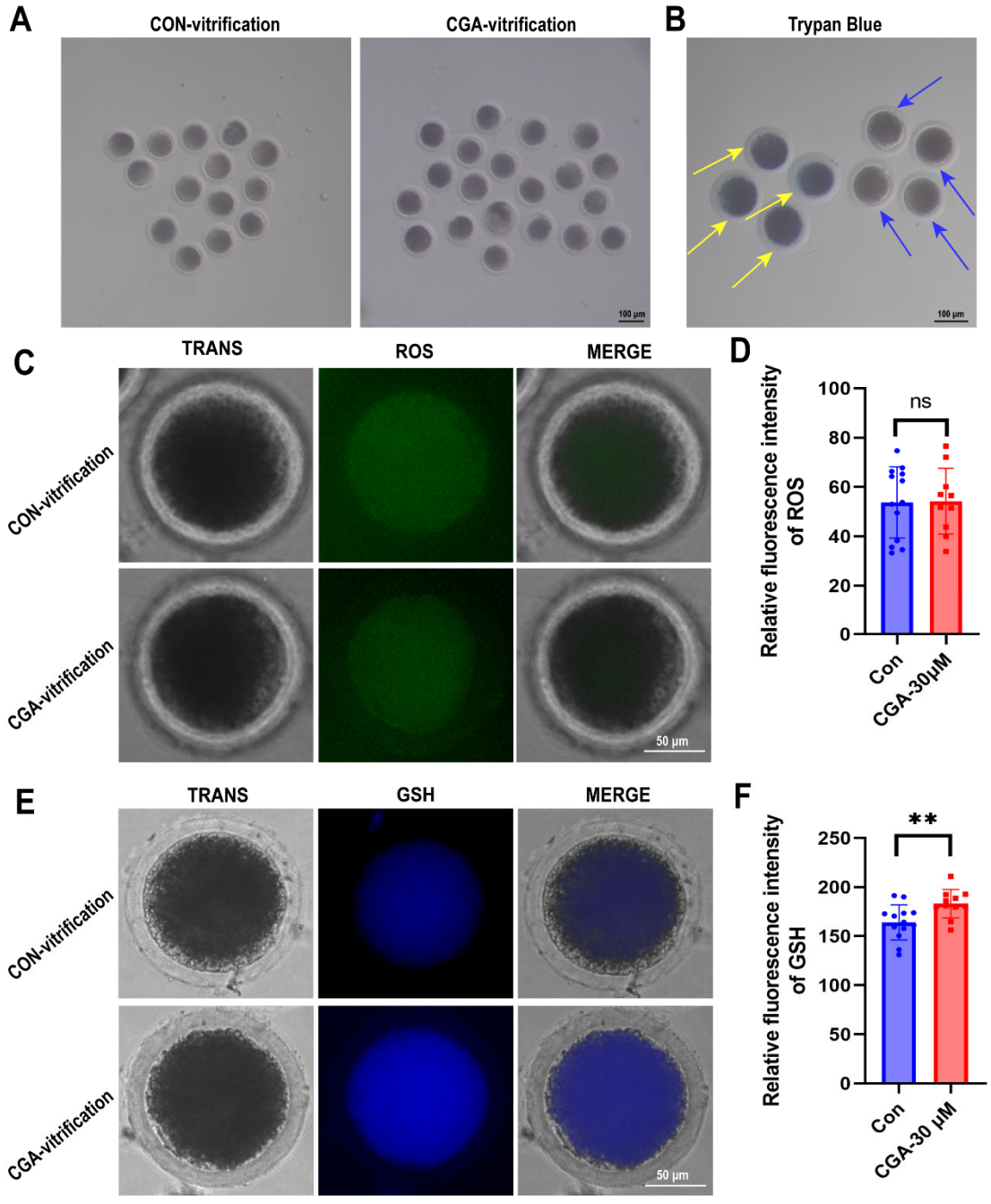


Figure 6. Effects of CGA on vitrification of porcine oocytes. (**A**) Morphological images of oocytes after vitrification and warming (scale bar = 100 μm). (**B**) Representative images of Trypan blue

staining of oocytes, with yellow arrows indicating dead cells and blue arrows indicating live cells (scale bar = 100 μm). This staining was used as an auxiliary verification for the primary morphological assessment. (**C**) Representative images of ROS staining in oocytes (scale bar = 50 μm). (**D**) Quantification of ROS fluorescence intensity (8–14 oocytes per group, $n = 3$). (**E**) Representative images of GSH staining in oocytes (scale bar = 50 μm). (**F**) Quantification of GSH fluorescence intensity (12–15 oocytes per group, $n = 3$), **, $p < 0.01$, ns, no significant difference ($p > 0.05$).

4. Discussion

Oocyte quality is a critical determinant of successful fertilization and subsequent embryonic development. During IVM, oocytes are highly susceptible to oxidative stress due to the marked differences between the culture environment and the physiological in vivo conditions, which severely compromise their maturational and developmental competence. To address this issue, researchers have supplemented various antioxidants into mammalian oocyte IVM systems and have led to significant improvement in oocyte quality [11,40,41]. In the present study, we evaluated the effects of CGA on the antioxidant status and developmental potential of porcine oocytes. Our results demonstrated that supplementation with 30 μM CGA during IVM significantly improved the oocyte maturation rate, which is consistent with previous reports on the beneficial effects of various antioxidants in farm animal oocyte maturation [42,43]. Notably, CGA treatment at various concentrations did not significantly affect the CEI in the present study, suggesting that the promoting effect of CGA on oocyte maturation may not depend on physical cumulus expansion [44]. In mammals, cumulus cell expansion is highly dependent on hyaluronic acid synthesis and the expression of extracellular matrix-related genes [45], whereas oocyte maturation relies more heavily on mitochondrial function and intracellular redox homeostasis. Previous studies have reported that supplementation with 50 μM CGA during IVM alleviates oxidative stress injury in porcine oocytes, accompanied by improved maturation, cleavage, and blastocyst rates [32]. This most promising concentration differs from that identified in our study. It should be noted that because the 20, 40, and 50 μM groups did not differ significantly from the control, and given the limited number of biological replicates, this finding should be interpreted cautiously. The discrepancy may be attributed to differences in the composition of the basal IVM culture system, including concentrations of small molecular components such as cysteine, sodium pyruvate, glucose, FSH, and LH. These components are known to modulate intracellular redox status and may influence the stability and bioavailability of CGA in the culture system, thereby affecting its biological efficacy.

To further elucidate the molecular mechanisms by which CGA enhances the IVM quality of porcine oocytes, we performed RNA-seq analysis. The results revealed marked transcriptomic differences between the control and CGA-supplemented groups, with DEGs predominantly enriched in pathways related to ribosome, OXPHOS, and thermogenesis. GO enrichment analysis further showed that the DEGs were mainly associated with translation, and ribosomal structural constituents. It is well established that meiotic resumption, cytoplasmic maturation, and early embryonic development in mammalian oocytes are highly dependent on selective translation of maternal mRNAs, with little involvement of de novo mRNA synthesis [46]. In the present study, genes in the ribosome pathway, such as *RPS26*, *RPL23A*, *RPS23*, *RPS27*, and *RPL23*, were upregulated following CGA treatment. These upregulated genes encode structural components of the small and large ribosomal subunits. Specifically, RPS26 is actively expressed in ovaries and oocytes and is involved in mouse follicular development and nucleolar transition; knockdown of *RPS26* leads to delayed follicular development and blocked nucleolar transition in mice [47]. In addition, *RPL23A* plays a crucial role in maintaining oocyte quality and function, and its knockdown leads to a decreased first polar body extrusion rate and abnormal chromosome alignment [48]. *RPS27* is enriched in mature oocytes, suggesting its involvement in maturation-related

translational processes [49]. Oocyte maturation is a highly protein synthesis-dependent event that requires sufficient ribosomes to support the translation of maternal mRNAs [50]. Therefore, the coordinated upregulation of these ribosome-related genes may reflect an increased cellular demand for ribosome biogenesis. However, it should be clearly noted that elevated mRNA levels only indicate altered transcriptional activity and do not directly demonstrate enhanced ribosome assembly efficiency or global translation rates. The functional link between these gene expression changes and CGA-promoted maturation still requires further confirmation through direct measurements of translational activity (e.g., puromycin incorporation assays) or functional validation of ribosome assembly.

Mitochondrial OXPHOS is the primary source of ATP production in oocytes, a process essential for spindle assembly, chromosome segregation, and subsequent embryonic development [51]. Meanwhile, OXPHOS not only serves as the core process for energy production but also constitutes a major source of ROS generation [52]. Notably, DEGs in our study were also significantly enriched in the OXPHOS pathway. Concurrently, OXPHOS pathway-related genes (e.g., *NDUFS8*, *NDUFB3*, *NDUFA13*, *NDUFAB1*, and *NDUFS6*) were upregulated in the CGA-treated group. The proteins encoded by these genes primarily localize to the inner mitochondrial membrane and constitute essential subunits of respiratory chain Complex I (NADH dehydrogenase). NDUFAB1 promotes follicle development by stimulating granulosa cell proliferation and inhibiting apoptosis, and is associated with the regulatory network of follicular growth [53]. As a transmembrane accessory subunit of Complex I, *NDUFB3* has been used as a key marker gene for assessing electron transport chain function and MMP in oocytes [54]. In addition, *NDUFA13*, *NDUFS8*, and *NDUFS6* also encode core or accessory subunits of Complex I. Specifically, the downregulation of NDUFA13 (also known as GRIM-19) has been demonstrated to reduce mouse oocyte viability, maturation, and subsequent embryo development [55]. These findings suggest that CGA treatment reflects an increased cellular demand for mitochondrial respiratory chain assembly and the maintenance of mitochondrial function in oocytes. However, the upregulation of gene expression does not directly prove that the assembly efficiency of Complex I or overall respiratory activity is enhanced. The functional link between these transcriptional changes and CGA-improved MMP still requires further verification through functional assays, such as direct measurements of Complex I activity, oxygen consumption rate, or ATP production.

To validate the reliability of our sequencing results, we further examined the expression of selected DEGs by qPCR. CGA treatment significantly upregulated the expression of *RPL30* (a ribosome-related gene) and *NDUFAB1* (an OXPHOS-related gene), which is consistent with the transcriptomic enrichment of ribosome and OXPHOS pathways. Additionally, *YWHAE* and *CHMP3* were also upregulated following CGA treatment. Previous studies have reported that multiple isoforms of the YWHA protein family are expressed in mouse oocytes and interact with CDC25B, a key cell cycle regulator [56]. CHMP3, a component of the ESCRT-III complex, is primarily involved in intracellular protein trafficking and membrane remodeling [57]. Collectively, these transcriptomic and qPCR findings suggest that CGA may exert multifaceted regulatory effects on porcine oocyte maturation. This is evidenced by changes in the expression of genes associated with protein synthesis, mitochondrial function, and cell cycle progression. However, we acknowledge certain limitations in this validation. First, while β-actin is a widely used reference gene, its stability under specific CGA treatment conditions was not systematically validated; therefore, the qPCR results should be strictly interpreted as the validation of expression trends. Second, these observations remain at the mRNA level, and the proposed functional enhancement of protein synthesis and mitochondrial bioenergetics requires direct functional validation in future studies.

Mammalian organisms possess an endogenous antioxidant defense system primarily comprising three key enzymes: superoxide dismutase, catalase, and glutathione peroxidase (GPX). Among these, GPX is primarily responsible for neutralizing intracellular hydrogen peroxide, thereby maintaining normal levels of ROS within cells [58]. During oocyte IVM, excessive accumulation of ROS can damage critical cellular DNA and proteins, exerting detrimental effects on oocyte quality and subsequent early embryonic development [59]. Numerous studies have demonstrated that supplementation with GSH during ovine oocyte IVM and vitrification alleviates oxidative stress, preserves mitochondrial function [60], reduces spindle damage [61], and improves oocyte developmental competence. In the present study, supplementation with 30 μM CGA significantly elevated intracellular GSH levels, indicating that CGA enhances the intracellular antioxidant reserve and helps maintain redox homeostasis. However, this increase was not accompanied by a detectable reduction in ROS levels. This discrepancy could be explained by several factors. First, GSH is a major non-enzymatic antioxidant that acts as a cellular redox buffer [62]. The elevated GSH levels may represent an enhanced "antioxidant reserve" induced by CGA, preparing the oocytes to cope with potential oxidative insults, rather than merely clearing an existing ROS burden. It is plausible that other antioxidant systems exhibited compensatory regulation, thus keeping ROS at a steady baseline level. Furthermore, we must acknowledge the limitations of the current assays. The DCFH-DA probe used for ROS detection primarily reflects global intracellular ROS. Given the extremely short half-life of ROS and the potential for compartmentalized ROS generation (such as in mitochondria), the sensitivity of the assay may be insufficient to capture subtle or localized fluctuations [63]. Additionally, we measured total GSH rather than the GSH/GSSG ratio, which is a more sensitive indicator of the cellular redox potential [64].

Mitochondria are essential organelles in mammalian oocytes, serving not only as sites of cellular energy metabolism but also playing a pivotal role during oocyte maturation. Mitochondrial dysfunction can compromise normal cellular development. Lee et al. [51] demonstrated that reduced MMP in porcine oocytes leads to decreased ATP production, impaired first polar body extrusion, and reduced blastocyst formation following parthenogenetic activation. In our study, 30 μM CGA significantly enhanced MMP and MitoTracker fluorescence intensity in mature porcine oocytes. It is important to note that these parameters serve as indirect readouts of MMP and mitochondrial mass, respectively. Additionally, because specific background subtraction was not applied during image analysis, these results should be interpreted as mitochondrial-associated fluorescence. Future studies utilizing direct functional assays (e.g., Seahorse extracellular flux analysis) are required to confirm actual changes in mitochondrial bioenergetics. In the present study, ROS levels in the control group oocytes were not markedly elevated. This may be attributable to the fact that the improvement in oocyte quality by CGA does not primarily depend on the suppression of early apoptosis. It suggested a relatively low level of oxidative damage, with apoptosis likely maintained at a basal level. In a study on ovine oocytes, 0.3% hydroxyapatite nanoparticles significantly reduced intracellular ROS levels and increased GSH levels, but had no effect on apoptosis [65]. Similarly, in a porcine oocyte heat-stress model (41.0 °C), CGA supplementation downregulated apoptosis levels, whereas under normal in vitro culture conditions (38.5 °C), apoptosis remained unaffected [28]. These findings suggest that the anti-apoptotic effect of CGA may only be triggered when cells are subjected to severe stress, and is difficult to detect under physiological or basal conditions.

Early embryonic development is influenced not only by oocyte quality but also by multiple factors, including sperm quality, fertilization conditions, and embryo culture systems. In addition, porcine IVF is inherently complicated by the issue of polyspermy, which adversely affects normal embryonic development [66]. In the present study, 30 μM

CGA did not significantly enhance either cleavage or blastocyst rates following IVF from fresh porcine oocytes. Given the limited number of independent IVF runs, it is possible that our study lacked sufficient statistical power to detect subtle, biologically meaningful differences in embryo development. Despite the observed improvement in these specific intracellular markers, the beneficial effects of CGA on subsequent embryonic development may be obscured by confounding factors inherent to the porcine IVF system, such as polyspermy, fertilization abnormalities, or fluctuations in culture conditions. However, because the polyspermy rate and specific sperm parameters were not directly measured in this study, these remain speculative possibilities. Previous studies have shown that 50 μM CGA improves MMP and ATP levels in porcine early parthenogenetic embryos, and promotes embryonic development by modulating oxidative stress and mitochondrial function [67]. In contrast to those reports, the present study employed a lower concentration (30 μM) of CGA, which was administered exclusively during the IVM phase. Importantly, the parthenogenetic model bypasses the issue of polyspermy, whereas our IVF system is heavily challenged by it. Accordingly, differences in CGA concentration, treatment regimen, and the developmental model may collectively account for the discrepancy between our findings and those of previous studies.

Oocyte vitrification is a primary method for preserving female germplasm resources. However, due to their high lipid content and cold sensitivity, porcine oocytes often exhibit mitochondrial dysfunction and reduced developmental competence after warming [68]. The low temperature, osmotic changes, and exposure to cryoprotectants during vitrification can induce ROS accumulation and disrupt redox homeostasis, thereby affecting the stability of cellular membranes, mitochondria, and the cytoskeleton [69]. CGA has been reported to reduce ROS levels, increase GSH content and MMP, and improve subsequent embryonic development in vitrified ovine oocytes [24]. In addition, antioxidant or mitochondrial protective compounds, such as resveratrol and metformin, have been shown to alleviate apoptosis, preserve mitochondrial function, and improve the developmental competence of vitrified porcine oocytes [70,71], highlighting the importance of limiting oxidative damage and maintaining mitochondrial homeostasis during oocyte cryopreservation. Notably, in the present study, supplementation with 30 μM CGA significantly increased short-term post-warming survival rate and intracellular GSH content of porcine oocytes after vitrification and warming, whereas intracellular ROS levels were not significantly affected. Moreover, CGA has been reported to increase intracellular GSH through regulation of the Nrf2 signaling pathway [72]. Because ROS generation during vitrification is influenced by multiple factors, including mitochondrial metabolic disturbances, cryoprotectant-induced cytotoxicity, and osmotic stress [73], CGA supplementation during the preceding maturation stage may not be sufficient to directly counteract all ROS generated during the subsequent vitrification process. Therefore, the present findings suggest a potential association between the beneficial effects of CGA on short-term post-warming survival and the enhancement of endogenous GSH-dependent antioxidant defenses. However, it is important to note that this study evaluated only short-term survival and did not assess the developmental competence of vitrified-warmed oocytes following IVF. Furthermore, because specific GSH synthesis inhibitors were not employed, whether the elevated GSH directly mediates this protective effect remains a hypothesis requiring further validation.

Although the present study revealed that 30 μM CGA improves porcine oocyte maturation quality, intracellular GSH levels, improves mitochondrial status, and enhances short-term post-warming survival. These beneficial effects are associated with changes in the expression of genes related to ribosome and OXPHOS pathways, several limitations remain. First, the IVF experiments were conducted exclusively using freshly matured oocytes. The developmental competence of vitrified-warmed oocytes following IVF was

not evaluated. Therefore, the improved short-term post-warming survival observed in this study cannot be extrapolated as a preservation of full developmental competence. Second, although we observed elevated GSH levels in vitrified-warmed oocytes, we did not employ specific GSH synthesis inhibitors in this study. Consequently, whether the elevated GSH directly mediates the improved post-warming survival remains a hypothesis that requires further validation. Third, CGA was supplemented only during in IVM and was not directly added to the equilibration solution, vitrification solution, or warming solution; therefore, whether CGA exerts direct protective effects during vitrification and warming remains unclear. Fourth, the sample size was limited, and the study was restricted to porcine oocytes without cross-species validation.

Future studies could employ overexpression, RNA interference, or specific pharmacological inhibitors/activators to further verify the functional roles of key genes in the ribosome and OXPHOS pathways during CGA treatment in porcine oocyte maturation and subsequent embryonic development. In addition, CGA could be added to vitrification or warming solutions to evaluate its protective effects and to determine the optimal concentration and exposure time. Furthermore, because the developmental competence of vitrified-warmed oocytes after IVF was not evaluated in this study, future research should focus on optimizing the IVF system to assess the post-warming developmental potential. The findings are currently limited to porcine oocytes and should be extrapolated with caution. However, because the ribosome and OXPHOS pathways are conserved and CGA is a bioactive natural compound, the results may be relevant to other mammalian species and human assisted reproductive technology (ART). Cross-species studies using bovine, ovine, and human oocytes should therefore be conducted to assess the conservation and generalizability of CGA effects, which would provide a more solid theoretical basis and technical support for livestock genetic resource conservation and the potential optimization of human ART.

5. Conclusions

In summary, supplementation of porcine oocyte IVM medium with 30 μM CGA enhances oocyte maturation rate, intracellular GSH levels, and improves mitochondrial status, thereby improving oocyte quality. These beneficial effects are associated with changes in the expression of genes related to ribosome and OXPHOS pathways. Furthermore, CGA improves short-term post-warming survival following vitrification. However, further studies are required to confirm whether this translates into preserved developmental competence. Collectively, our findings provide a theoretical foundation for optimizing mammalian oocyte IVM systems and warrant future investigation into optimizing vitrification preservation.

Supplementary Materials: The following supporting information can be downloaded at: https://www.mdpi.com/article/10.3390/antiox15111482/s1, Figure S1: KEGG enrichment analysis under stringent criteria; Table S1: Sequencing Data Quality Control; Table S2: Number of DEGs; Table S3: KEGG Enrichment Analysis; Table S4: Number of validated DEGs under stringent criteria; Table S5: GO Enrichment Analysis.

Author Contributions: Writing—original draft, K.S.; Visualization, L.W., Y.K. and K.L.; Supervision, F.Y., Q.M. and Y.K.; Investigation, F.Y. and K.L.; Formal analysis, Q.M., X.H. and L.W.; Project administration, X.H. and X.L.; Conceptualisation, X.L. and T.Y.; Funding acquisition, X.L.; Writing—review and editing, S.G., X.L. and T.Y. All authors have read and agreed to the published version of the manuscript.

Funding: This research was funded by the National Key R&D Program of China (2023YFF0724704) and the Pig Industry Technology System Innovation Team Project of Henan Province (HARS-22-12-G4). Agricultural Breeds Research Project of Henan Province (2026020202).

Institutional Review Board Statement: This study was approved by the Henan Agricultural University Animal Care and Use Committee. Ethical approval was granted on 10 March 2025 (approval number: HNND2025031352).

Informed Consent Statement: Not applicable.

Data Availability Statement: The original contributions presented in this study are included in the article/Supplementary Materials. Further inquiries can be directed to the corresponding author(s). All raw sequencing data generated in this study have been deposited in the NCBI and are accessible through accession number PRJNA1552808. The data are currently under embargo due to ongoing patent application and will be publicly released on 31 December 2027.

Conflicts of Interest: The authors declare no conflicts of interest.

References

1. Song, K.; Lee, E. Modification of maturation condition improves oocyte maturation and in vitro development of somatic cell nuclear transfer pig embryos. *J. Vet. Sci.* **2007**, *8*, 81–87. [CrossRef] [PubMed]
2. Liu, M.; Cui, J.; Chang, H.-M.; Liu, J.; Leung, P.C.K. Advances in human oocyte in vitro maturation: Current status and future perspectives: A narrative review. *Reprod. Fertil.* **2025**, *6*, e250092. [CrossRef] [PubMed]
3. Saragusty, J.; Arav, A. Current progress in oocyte and embryo cryopreservation by slow freezing and vitrification. *Reproduction* **2011**, *141*, 1–19. [CrossRef] [PubMed]
4. Rall, W.F.; Fahy, G.M. Ice-free cryopreservation of mouse embryos at -196 degrees C by vitrification. *Nature* **1985**, *313*, 573–575. [CrossRef] [PubMed]
5. Yang, Q.Y.; Zhu, L.X.; Wang, M.; Huang, B.; Li, Z.; Hu, J.; Xi, Q.S.; Liu, J.; Jin, L. Analysis of maturation dynamics and developmental competence of in vitro matured oocytes under time-lapse monitoring. *Reprod. Biol. Endocrinol.* **2021**, *19*, 183. [CrossRef] [PubMed]
6. Souza-Fabjan, J.M.G.; Leal, G.R.; Monteiro, C.A.S.; Batista, R.; Barbosa, N.O.; Freitas, V.J.F. In vitro embryo production in small ruminants: What is still missing? *Anim. Reprod.* **2023**, *20*, e20230055. [CrossRef] [PubMed]
7. Zhu, Y.; Liu, H.; Zheng, L.; Luo, Y.; Zhou, G.; Li, J.; Hou, Y.; Fu, X. Vitrification of Mammalian Oocytes: Recent Studies on Mitochondrial Dysfunction. *Biopreserv. Biobank.* **2024**, *22*, 428–440. [CrossRef] [PubMed]
8. Chang, C.C.; Shapiro, D.B.; Nagy, Z.P. The effects of vitrification on oocyte quality. *Biol. Reprod.* **2022**, *106*, 316–327. [CrossRef] [PubMed]
9. Blancas-Alvarez, L.A.; Alvarez-Guerrero, A.L.; Alcantar-Rodriguez, A.; Medrano, A. Effects of melatonin on in vitro oocyte maturation and embryo development in pigs. *Vet. World* **2025**, *18*, 1234–1241. [CrossRef] [PubMed]
10. Kwak, S.S.; Cheong, S.A.; Jeon, Y.; Lee, E.; Choi, K.C.; Jeung, E.B.; Hyun, S.H. The effects of resveratrol on porcine oocyte in vitro maturation and subsequent embryonic development after parthenogenetic activation and in vitro fertilization. *Theriogenology* **2012**, *78*, 86–101. [CrossRef] [PubMed]
11. Chen, F.; Wang, H.; Liu, Y.; Liu, Q.; Yang, S.; Ma, Z.; Yuan, Y.G. Taurine promotes porcine oocyte maturation and embryonic development by reducing oxidative stress and enhancing energy metabolism. *Theriogenology* **2026**, *251*, 117756. [CrossRef] [PubMed]
12. Li, L.; Han, Q.; Chen, Y.; Zhang, M.; Wang, L.; An, X.; Zhang, S.; Zhai, Y.; Dai, X.; Tang, B.; et al. β-nicotinamide mononucleotide rescues the quality of aged oocyte and improves subsequent embryo development in pigs. *PLoS ONE* **2023**, *18*, e0291640. [CrossRef] [PubMed]
13. Stalmach, A.; Steiling, H.; Williamson, G.; Crozier, A. Bioavailability of chlorogenic acids following acute ingestion of coffee by humans with an ileostomy. *Arch. Biochem. Biophys.* **2010**, *501*, 98–105. [CrossRef] [PubMed]
14. Zhao, Y.Y.; Wang, J.K.; Ballevre, O.; Luo, H.L.; Zhang, W.G. Antihypertensive effects and mechanisms of chlorogenic acids. *Hypertens. Res.* **2012**, *35*, 370–374. [CrossRef] [PubMed]
15. Yao, Y.X.; Yao, C.H.; Zhang, C.Y.; Peng, X.Z.; Dai, S.; Yu, Y.J.; Li, Y.Z.; Zhang, S.L.; Li, Y.X. Chlorogenic Acid Ameliorates Acetaminophen-Induced Liver Injury Through AMPK/mTOR/ULK1-Mediated Autophagy Activation. *Am. J. Chin. Med.* **2025**, *53*, 523–542. [CrossRef] [PubMed]
16. Ouyang, H.; Miao, H.; Zhang, H.; Lu, B.; Zhang, J.Y.; Zhang, T.Y.; Zhu, J.F.; Wang, Z.T.; Ji, L.L. Chlorogenic Acid Alleviates Non-Alcoholic Steatohepatitis via Suppressing Liver Inflammatory Injury by Targeting Transforming Growth Factor Beta Receptor-1 in Liver Sinusoidal Endothelial Cells. *Phytother. Res.* **2025**, *39*, 5316–5344. [CrossRef] [PubMed]
17. Wei, M.J.; Gu, X.N.; Li, H.; Zheng, Z.Y.; Qiu, Z.M.; Sheng, Y.C.; Lu, B.; Wang, Z.T.; Ji, L.L. EGR1 is crucial for the chlorogenic acid-provided promotion on liver regeneration and repair after APAP-induced liver injury. *Cell Biol. Toxicol.* **2023**, *39*, 2685–2707. [CrossRef] [PubMed]

18. Qin, Y.M.; Wang, S.Q.; Huang, W.W.; Li, K.J.; Wu, M.; Liu, W.L.; Han, J.Z. Chlorogenic acid improves intestinal morphology by enhancing intestinal stem-cell activity. *J. Sci. Food Agric.* **2023**, *103*, 3287–3294. [CrossRef] [PubMed]
19. Song, S.J.; Choi, S.; Park, T. Decaffeinated green coffee bean extract attenuates diet-induced obesity and insulin resistance in mice. *Evid. Based Complement Altern. Med.* **2014**, *2014*, 718379. [CrossRef] [PubMed]
20. Zeng, X.; Chen, L.; Zheng, B. Extrusion and chlorogenic acid treatment increase the ordered structure and resistant starch levels in rice starch with amelioration of gut lipid metabolism in obese rats. *Food Funct.* **2024**, *15*, 5224–5237. [CrossRef] [PubMed]
21. Huang, K.; Liang, X.C.; Zhong, Y.L.; He, W.Y.; Wang, Z. 5-Caffeoylquinic acid decreases diet-induced obesity in rats by modulating PPARα and LXRα transcription. *J. Sci. Food Agric.* **2015**, *95*, 1903–1910. [CrossRef] [PubMed]
22. Shirkhani, S.; Marandi, S.M.; Nasr-Esfahani, M.H.; Kim, S.K. Effects Of Exercise Training And Chlorogenic Acid Supplementation On Hepatic Lipid Metabolism In Prediabetes Mice. *Diabetes Metab. J.* **2023**, *47*, 771–783. [CrossRef] [PubMed]
23. Zhang, S.X.; Wang, D.L.; Qi, J.J.; Yang, Y.W.; Sun, H.; Sun, B.X.; Liang, S. Chlorogenic acid ameliorates the heat stress-induced impairment of porcine Sertoli cells by suppressing oxidative stress and apoptosis. *Theriogenology* **2024**, *214*, 148–156. [CrossRef] [PubMed]
24. Tao, H.; Zhao, Y.; Zhang, Q.; Li, X.; Hu, G.; Wang, Y.; Zeng, W. Effects of Chlorogenic Acid on In Vitro Maturation and Vitrification Cryopreservation of Sheep Oocytes. *Vet. Sci.* **2025**, *12*, 62. [CrossRef] [PubMed]
25. Signorini, C.; Corsaro, R.; Collodel, G.; Maettner, R.; Sterzik, K.; Strehler, E.; Liguori, L.; Moretti, E. Addition of Chlorogenic Acid to Human Semen: Effects on Sperm Motility, DNA Integrity, Oxidative Stress, and Expression. *Antioxidants* **2025**, *14*, 382. [CrossRef] [PubMed]
26. Wang, Y.H.; Zhang, L.M.; Sohail, T.; Kang, Y.; Sun, X.M.; Li, Y.J. Chlorogenic Acid Improves Quality of Chilled Ram Sperm by Mitigating Oxidative Stress. *Animals* **2022**, *12*, 163. [CrossRef] [PubMed]
27. Namula, Z.; Hirata, M.; Wittayarat, M.; Tanihara, F.; Nguyen, N.T.; Hirano, T.; Nii, M.; Otoi, T. Effects of chlorogenic acid and caffeic acid on the quality of frozen-thawed boar sperm. *Reprod. Domest. Anim.* **2018**, *53*, 1600–1604. [CrossRef] [PubMed]
28. Nguyen, T.V.; Do, L.T.K.; Somfai, T.; Otoi, T.; Taniguchi, M.; Kikuchi, K. Presence of chlorogenic acid during in vitro maturation protects porcine oocytes from the negative effects of heat stress. *Anim. Sci. J.* **2019**, *90*, 1530–1536. [CrossRef] [PubMed]
29. Nguyen, T.V.; Wittayarat, M.; Do, L.T.K.; Nguyen, T.V.; Nii, M.; Namula, Z.; Kunihara, T.; Tanihara, F.; Hirata, M.; Otoi, T. Effects of chlorogenic acid (CGA) supplementation during in vitro maturation culture on the development and quality of porcine embryos with electroporation treatment after in vitro fertilization. *Anim. Sci. J.* **2018**, *89*, 1207–1213. [CrossRef] [PubMed]
30. Van Nguyen, T.; Do, L.T.K.; Nguyen, N.-A.T.; Kikuchi, K.; Somfai, T.; Otoi, T. The Effects of an In Vitro Oocyte Maturation System and Chlorogenic Acid Supplementation during Embryo Culture on the Development of Porcine Cloned Embryos Derived from Native Vietnamese Ban Pigs. *Vet. Med. Int.* **2023**, *2023*, 5702970. [CrossRef] [PubMed]
31. Thongkittidilok, C.; Le, Q.A.; Lin, Q.; Takebayashi, K.; Do, T.K.L.; Namula, Z.; Hirata, M.; Tanihara, F.; Otoi, T. Effects of individual or in-combination antioxidant supplementation during in vitro maturation culture on the developmental competence and quality of porcine embryos. *Reprod. Domest. Anim.* **2022**, *57*, 314–320. [CrossRef] [PubMed]
32. Nguyen, T.V.; Tanihara, F.; Do, L.; Sato, Y.; Taniguchi, M.; Takagi, M.; Van Nguyen, T.; Otoi, T. Chlorogenic acid supplementation during in vitro maturation improves maturation, fertilization and developmental competence of porcine oocytes. *Reprod. Domest. Anim.* **2017**, *52*, 969–975. [CrossRef] [PubMed]
33. Ren, J.; Ding, Y.; Shi, J.; Gu, S.; Luo, L.; Feng, Z.; Gu, T.; Xu, Z.; Huang, S.; Li, Z.; et al. Porcine Granulosa-Cell-Derived Exosomes Enhance Oocyte Development: An In Vitro Study. *Antioxidants* **2024**, *13*, 348. [CrossRef] [PubMed]
34. Lu, T.; Ma, X.; Wang, M.; Pan, Y.; Yang, X.; Qiu, S.; Yang, X.; Yu, S. Curcumin-Loaded Milk-Derived Exosomes Improve the Developmental Competence of Yak Oocytes by Regulating Mitophagy. *Antioxidants* **2026**, *15*, 922. [CrossRef] [PubMed]
35. Li, R.Q.; Li, Y.R.; Kristiansen, K.; Wang, J. SOAP: Short oligonucleotide alignment program. *Bioinformatics* **2008**, *24*, 713–714. [CrossRef] [PubMed]
36. Kim, D.; Landmead, B.; Salzberg, S.L. HISAT: A fast spliced aligner with low memory requirements. *Nat. Methods* **2015**, *12*, 357–360. [CrossRef] [PubMed]
37. Langmead, B.; Salzberg, S.L. Fast gapped-read alignment with Bowtie 2. *Nat. Methods* **2012**, *9*, 357–359. [CrossRef] [PubMed]
38. Li, B.; Dewey, C.N. RSEM: Accurate transcript quantification from RNA-Seq data with or without a reference genome. *BMC Bioinform.* **2011**, *12*, 323. [CrossRef] [PubMed]
39. Love, M.I.; Huber, W.; Anders, S. Moderated estimation of fold change and dispersion for RNA-seq data with DESeq2. *Genome Biol.* **2014**, *15*, 550. [CrossRef]
40. Feng, Z.; Song, J.; Lin, C.; Wu, S.; Wang, Y.; Hui, Q.; Pan, Y.; Zou, Y.; Zeng, C.; Guo, J.; et al. Enhancing porcine oocyte quality and embryo development through natural antioxidants. *Theriogenology* **2025**, *232*, 96–108. [CrossRef] [PubMed]
41. Okamoto, N.; Sato, Y.; Kawagoe, Y.; Kawamura, K. Pterostilbene enhances reproductive outcomes and oocyte quality in aged mice without adverse effects. *Aging* **2025**, *17*, 1762–1783. [CrossRef] [PubMed]
42. Lim, E.S.; Lee, S.E.; Park, M.J.; Han, D.H.; Lee, H.B.; Ryu, B.; Kim, E.Y.; Park, S.P. Piperine improves the quality of porcine oocytes by reducing oxidative stress. *Free Radic. Biol. Med.* **2024**, *213*, 1–10. [CrossRef] [PubMed]

43. Chen, Q.; Gao, L.; Li, J.; Yuan, Y.; Wang, R.; Tian, Y.; Lei, A. A-Ketoglutarate Improves Meiotic Maturation of Porcine Oocytes and Promotes the Development of PA Embryos, Potentially by Reducing Oxidative Stress through the Nrf2 Pathway. *Oxid. Med. Cell. Longev.* **2022**, *2022*, 7113793. [CrossRef] [PubMed]
44. Redel, B.K.; Spate, L.D.; Yuan, Y.; Murphy, C.N.; Roberts, R.M.; Prather, R.S. Neither gonadotropin nor cumulus cell expansion is needed for the maturation of competent porcine oocytes in vitro. *Biol. Reprod.* **2021**, *105*, 533–542. [CrossRef] [PubMed]
45. Sato, E.; Yokoo, M. Morphological and biochemical dynamics of porcine cumulus-oocyte complexes: Role of cumulus expansion in oocyte maturation. *Ital. J. Anat. Embryol. Arch. Ital. DI Anat. Ed. Embriol.* **2005**, *110*, 205–217.
46. Conti, M.; Kunitomi, C. A genome-wide perspective of the maternal mRNA translation program during oocyte development. *Semin. Cell Dev. Biol.* **2024**, *154*, 88–98. [CrossRef] [PubMed]
47. Liu, X.M.; Yan, M.Q.; Ji, S.Y.; Sha, Q.Q.; Huang, T.; Zhao, H.; Liu, H.B.; Fan, H.Y.; Chen, Z.J. Loss of oocyte Rps26 in mice arrests oocyte growth and causes premature ovarian failure. *Cell Death Dis.* **2018**, *9*, 1144. [CrossRef] [PubMed]
48. Han, Y.; Du, Z.; Wu, H.; Zhao, R.; Liu, J.; Gao, S.; Zeng, S. CALB1 and RPL23 Are Essential for Maintaining Oocyte Quality and Function During Aging. *Aging Cell* **2025**, *24*, e14466. [CrossRef] [PubMed]
49. Kandil, O.M.; Ghanem, N.; Abdoon, A.S.; Hölker, M.; Phatsara, C.; Schellander, K.; Tesfaye, D. Transcriptional analysis of buffalo (Bubalus bubalis) oocytes during in vitro maturation using bovine cDNA microarray. *Reprod. Domest. Anim.* **2010**, *45*, 63–74. [CrossRef] [PubMed]
50. Danielson, K.J.; Judson, K.L.; Greenblatt, E.J. Reproductive Ageing: Declining translational capacity as a potential driver for oocyte meiotic instability. *Reproduction* **2024**, *168*, e240198. [CrossRef] [PubMed]
51. Lee, S.K.; Zhao, M.H.; Kwon, J.W.; Li, Y.H.; Lin, Z.L.; Jin, Y.X.; Kim, N.H.; Cui, X.S. The association of mitochondrial potential and copy number with pig oocyte maturation and developmental potential. *J. Reprod. Dev.* **2014**, *60*, 128–135. [CrossRef] [PubMed]
52. Roth, Z. Symposium review: Reduction in oocyte developmental competence by stress is associated with alterations in mitochondrial function. *J. Dairy Sci.* **2018**, *101*, 3642–3654. [CrossRef] [PubMed]
53. Sun, X.; Chen, X.; Zhao, J.; Ma, C.; Yan, C.; Liswaniso, S.; Xu, R.; Qin, N. Transcriptome comparative analysis of ovarian follicles reveals the key genes and signaling pathways implicated in hen egg production. *BMC Genom.* **2021**, *22*, 899. [CrossRef] [PubMed]
54. Yan, Y.; Zhang, H.; Xu, R.; Luo, L.; Yin, L.; Wu, H.; Zhang, Y.; Li, C.; Lu, S.; Tang, Y.; et al. Single-cell sequencing reveals the transcriptional alternations of 17β-estradiol suppressing primordial follicle formation in neonatal mouse ovaries. *Cell Prolif.* **2024**, *57*, e13713. [CrossRef] [PubMed]
55. Chao, L.; Wang, X.; Yang, Y.; Cui, W.; Xu, J.; Chen, H.; Hao, A.; Deng, X. Downregulation of gene expression and activity of GRIM-19 affects mouse oocyte viability, maturation, embryo development and implantation. *J. Assist. Reprod. Genet.* **2015**, *32*, 461–470. [CrossRef] [PubMed]
56. Eisa, A.A.; De, S.; Detwiler, A.; Gilker, E.; Ignatious, A.C.; Vijayaraghavan, S.; Kline, D. YWHA (14-3-3) protein isoforms and their interactions with CDC25B phosphatase in mouse oogenesis and oocyte maturation. *BMC Dev. Biol.* **2019**, *19*, 20. [CrossRef] [PubMed]
57. Muzioł, T.; Pineda-Molina, E.; Ravelli, R.B.; Zamborlini, A.; Usami, Y.; Göttlinger, H.; Weissenhorn, W. Structural basis for budding by the ESCRT-III factor CHMP3. *Dev. Cell* **2006**, *10*, 821–830. [CrossRef] [PubMed]
58. Bahety, D.; Böke, E.; Rodríguez-Nuevo, A. Mitochondrial morphology, distribution and activity during oocyte development. *Trends Endocrinol. Metab.* **2024**, *35*, 902–917. [CrossRef] [PubMed]
59. Ren, J.; Liu, G.; Cui, H.; Dong, X.; Mao, S.; Liu, Y.; Dai, Y. Effect of glutathione addition on vitrification of ovine oocytes. *Theriogenology* **2025**, *240*, 117412. [CrossRef] [PubMed]
60. Ren, J.; Hao, Y.; Liu, Z.; Li, S.; Wang, C.; Wang, B.; Liu, Y.; Liu, G.; Dai, Y. Effect of exogenous glutathione supplementation on the in vitro developmental competence of ovine oocytes. *Theriogenology* **2021**, *173*, 144–155. [CrossRef] [PubMed]
61. Al-Zubaidi, U.; Liu, J.; Cinar, O.; Robker, R.L.; Adhikari, D.; Carroll, J. The spatio-temporal dynamics of mitochondrial membrane potential during oocyte maturation. *Mol. Hum. Reprod.* **2019**, *25*, 695–705. [CrossRef] [PubMed]
62. Curnow, E.C.; Ryan, J.; Saunders, D.; Hayes, E.S. Bovine in vitro oocyte maturation as a model for manipulation of the gamma-glutamyl cycle and intraoocyte glutathione. *Reprod. Fertil. Dev.* **2008**, *20*, 579–588. [CrossRef] [PubMed]
63. Amoushahi, M.; Lykke-Hartmann, K. Distinct Signaling Pathways Distinguish in vivo From in vitro Growth in Murine Ovarian Follicle Activation and Maturation. *Front. Cell Dev. Biol.* **2021**, *9*, 708076. [CrossRef] [PubMed]
64. Petrova, B.; Liu, K.; Tian, C.; Kitaoka, M.; Freinkman, E.; Yang, J.; Orr-Weaver, T.L. Dynamic redox balance directs the oocyte-to-embryo transition via developmentally controlled reactive cysteine changes. *Proc. Natl. Acad. Sci. USA* **2018**, *115*, E7978–E7986. [CrossRef] [PubMed]
65. Zhou, G.; Liu, A.; Li, J.; Bai, J.; Liu, Y.; Liu, Q.; Wang, J.; Liu, C.; Guo, Y.; Wan, P.; et al. Hydroxyapatite Nanoparticles Enhance In Vitro Maturation of Sheep Oocytes by Attenuating Oxidative Stress. *ACS Appl. Nano Mater.* **2025**, *8*, 11976–11985. [CrossRef]
66. Garcia-Canovas, M.; Parrilla, I.; Cuello, C.; Gil, M.A.; Martinez, E.A. Swine in vitro embryo production: Potential, challenges, and advances. *Anim. Reprod. Sci.* **2024**, *270*, 107600. [CrossRef] [PubMed]

67. Qu, H.X.; Wang, Y.Q.; Dong, Y.W.; Qi, J.J.; Wei, H.K.; Zhang, Y.; Sun, H.; Sun, B.X.; Liang, S. Chlorogenic acid improves the development of porcine parthenogenetic embryos by regulating oxidative stress and ameliorating mitochondrial function. *Reprod. Domest. Anim.* **2024**, *59*, e14596. [CrossRef] [PubMed]
68. Xu, J.; Sun, L.; Wu, C.; Zhang, S.; Ju, S.; Rui, R.; Zhang, D.; Dai, J. Involvement of PINK1/Parkin-mediated mitophagy in mitochondrial functional disruption under oxidative stress in vitrified porcine oocytes. *Theriogenology* **2021**, *174*, 160–168. [CrossRef] [PubMed]
69. Cao, B.; Qin, J.; Pan, B.; Qazi, I.H.; Ye, J.; Fang, Y.; Zhou, G. Oxidative Stress and Oocyte Cryopreservation: Recent Advances in Mitigation Strategies Involving Antioxidants. *Cells* **2022**, *11*, 3573. [CrossRef] [PubMed]
70. Ito, J.; Shirasuna, K.; Kuwayama, T.; Iwata, H. Resveratrol treatment increases mitochondrial biogenesis and improves viability of porcine germinal-vesicle stage vitrified-warmed oocytes. *Cryobiology* **2020**, *93*, 37–43. [CrossRef] [PubMed]
71. Zhou, D.; Liu, H.; Zheng, L.; Liu, A.; Zhuan, Q.; Luo, Y.; Zhou, G.; Meng, L.; Hou, Y.; Wu, G.; et al. Metformin alleviates cryoinjuries in porcine oocytes by reducing membrane fluidity through the suppression of mitochondrial activity. *Commun. Biol.* **2024**, *7*, 925. [CrossRef] [PubMed]
72. Yao, J.; Peng, S.; Xu, J.; Fang, J. Reversing ROS-mediated neurotoxicity by chlorogenic acid involves its direct antioxidant activity and activation of Nrf2-ARE signaling pathway. *BioFactors* **2019**, *45*, 616–626. [CrossRef] [PubMed]
73. Song, K.; Wang, L.; Yang, F.; Zhu, H.; Meng, Q.; Han, X.; Qiao, R.; Bai, J.; Gun, S.; Yu, T.; et al. Research Progress on Mammalian Oocyte Vitrification: From Damage Mechanisms to Optimization Strategies. *Animals* **2026**, *16*, 1406. [CrossRef] [PubMed]

Disclaimer/Publisher's Note: The statements, opinions and data contained in all publications are solely those of the individual author(s) and contributor(s) and not of MDPI and/or the editor(s). MDPI and/or the editor(s) disclaim responsibility for any injury to people or property resulting from any ideas, methods, instructions or products referred to in the content.